Glacial Isostatic Adjustment Contributions to Sea-Level Changes

The GIA-effect of historic, recent and future mass-changes of the Greenland ice-sheet and it's effect on relative sea level

Master's Thesis

Carsten Ankjær Ludwigsen
June 2016

DTU Space
National Space Institute

Abstract

The sea level equation (SLE) by Spada and Stocchi 2006 [26] gives the change rate of the relative sea level (RSL) induced by glacial isostatic adjustment (GIA) of melting ice mass on land, also called sea level 'fingerprints'. The effect of the viscoelastic rebound induced by the last deglaciation, as seen when solving the SLE using the ICE-5G model glaciation chronology (Peltier, 2004 [22]) dating back to the last glacial maximum (LGM), is still today causing large fingerprints in particular in Scandinavia and North America, effecting the sea level with rates up to 15 mm/yr. The same calculations are applied to present ice loss observed by GRACE and for four projections of the Greenland ice sheet (GrIS) for the 21st century. For the current ice melt, the GIA-contribution to RSL is 0.1 mm/yr at Greenlands coastline, and 5×10^{-4} mm/yr in a far field case (region around Denmark). For the GrIS-projections, the same result in 2100 is 1 mm/yr and up to 0.01 mm/yr, respectively. In agreement with the GrIS contribution to RSL from other studies (Bamber and Riva, 2010 [1], Spada et al, 2012 [28]) this study finds that the GIA-contribution of present or near-future (within 21st century) change of the GrIS to RSL is not relevant when discussing adaptation to near-future sea level changes.

Abbreviations

BP	Before present
DIL	Dynamic ice loss
ENSO	El Niño Southern Oscillation
ESL	Eustatic sea level
EWH	Equivalent Water Height
GF	Greens Functions
GIA	Glacial Isostatic Adjustment
GMSL	Global Mean Sea Level
GRACE	Gravity Recovery And Climate Experiment
GrIS	Greenland ice sheet
ICE-5G	Fifth generation of ice history model since LGM by Peltier, 2004[22]
ICE-GR	Ice model based on GRACE-observations
IM45	Ice history model based on SMB-projections forced with RCP 4.5
IM85	Ice history model based on SMB-projections forced with RCP 8.5
IMGRa	Ice history model based on accelerated GRACE-projections
IMGRt	Ice history model based on linear GRACE-projections
IPCC	Intergovernmental Panel of Climate Change
LDC's	Load Deformation Coefficients
LF	Land function
LGM	Last Glacial Maximum (21 kyr's ago)
MB	Mass balance
NAO	North Atlantic Oscillation
OF	Ocean function
RCP	Representative Concentration Pathways
RSL	Relative sea level
SELEN	SEa Level EquatioN solver
SLC	Sea level change
SLE	Sea level equation
SMB	Surface mass balance

Constants

Oceanic area	A_O	3.62×10^8 km^2
Density of ocean water	ρ_w	1029 kg m^{-3}
Density of ice	ρ_i	917 kg m^{-3}
Gravitational constant	G	6.674×10^{-11} Nm^2 kg^{-2}

List of Figures

1.0.1 Local sea level trends determined for a finite period (1993 - 2016) by altimeter data. They reflect the impact of decadal scale climate variability and local sea surface height trends, which includes crustal displacements, glacial isostatic adjustment (GIA), steric effects, and even change in local wind patterns. Source: `http://sealevel.colorado.edu/content/map-sea-level-trends` 6

1.2.1 Global mean sea level from 1993 to 2016 as estimated from satellite altimeter data. The average trend for the period i 3.4 ±0.4 mm/yr. Taken from `sealevel.colorado.edu` . . . 8

1.2.2 Processes affecting relative and eustatic sea-level. World Climate Research Programme, 2011. 10

1.3.1 Local sea level trends determined for a finite period (1992 - 2013) by altimeter data. Source: `http://sealevel.colorado.edu/content/map-sea-level-trends` 11

1.3.2 Relative sea-level change rates from present change of ice masses. The green line indicates the ice sheet's contribution to eustatic sea level change rate (1.4 mm/yr). From Bamber and Riva (2010) 13

2.1.1 The solid Earth's response during peak glaciation and deglaciation. From: `gsc.nrcan.gc.ca/geodyn/images/` 15

2.3.1 Surface elevation change and mass balance of GrIS. The total MB, SMB and DIL is shown for the periods 1900-1983 (left), 1983-2003 (middle) and 2003-2010 (right). From Kjeldsen et al (2015)[11]. 20

3.1.1 A simplified spherical earth model. Denotions of depth-range do not necessarily align with the depth range used in the VM2-model and their size is not in-scale. From Sørensen et al. (2010). 22

3.2.1 ICE-5G total elevation change from 21 kyr to present. 24

3.2.2 Monthly and yearly mass-loss obtained from GRACE-observations for GrIS relative to 2008. The average mass loss is 206 ± 68 Gt/yr. The yearly mass loss is obtained by the Jan-to-Jan difference. 26

3.2.3 Total elevation change from 2003-2014 of the ICE-GR model, obtained by GRACE-measurements. 27

3.3.1 The yearly GrIS mass loss of the 4 projections as well as for SMB and DIL for IM45 and IM85. The original GRACE observations (from 2003 to 2014) of GrIS. 29

3.3.2 Trend and acceleration from GRACE-data between 2003-2014 for GrIS. 30

3.3.3 Projected elevation change (water equivalent) for Greenland in 2100. Left for IMGRt and right for IMGRa. 30

3.3.4 Average SMB trends from raw data for the RCP4.5 (top) and RCP8.5 (bottom), for the period 2031-2050 (left) and 2081-2100 (right) and their corresponding average mass change (mass gain). 32

3.3.5 Average mass balance (left), surface mass balance (middle) and dynamic ice loss (right) obtained by Hirham (SMB) and GRACE (MB) for the years 2003-2010. DIL is the difference between the two. 34

3.3.6 Mass balance (top), surface mass balance (middle) and dynamic ice loss (bottom) for ice histories of IM45 (left column) and IM85 (right column). The number above the maps, is the contribution of average mass loss from 1990 to 2100 (see also figure 3.3.1). 35

4.1.1 Present-day GIA-induced fingerprints from ICE-5G (21 kyr BP - present), as obtained by SELEN. The corresponding eustatic sea level change is in total 127.1 m (on average 5.8 mm/yr) (see also figure 4.1.4) 39

4.1.2 GIA-induced fingerprints from ICE-GR (2003-2014), as obtained by SELEN. The corresponding eustatic sea level change is in total 6.8 mm (on average 0.56 mm/yr) (see also figure 4.1.4) 40

4.1.3 The present-day vertical uplift (top, $\dot{U}$) and geoid change rate (bottom, $\dot{N}$), for the ICE-5G model (left) and ICE-GR (right). 41

4.1.4 ESL-change and the change-rate for ICE-5G and ICE-GR as given by SELEN relative to present. The total ESL-change for ICE-5G is 127.1 m and for 6.8 mm ICE-GR. 42

4.2.1 *Top left*: the total elevation change for GrIS for the ice history of **IMGRt** from 1990 to 2100. *Top right and bottom panel*: The relative sea level change (mm/yr, different scaled colorbars) in 2100 for IMGRt obtained by the GIA-predictions from SELEN around Greenland (top right), around Scandinavia (bottom left) and the whole world (bottom right). The corresponding total eustatic sea level change for the period is, according to the SELEN-output, 110.9 mm, or on average 1.01 mm/yr. 44

4.2.2 Same as in figure 4.2.1, but for the **IMGRa** ice model. The corresponding total eustatic sea level change for the period is, according to the SELEN-output, 102.6 mm, or on average 0.93 mm/yr. 45

4.2.3 Same as in figure 4.2.1, but for the **IM45** ice model. The corresponding total eustatic sea level change for the period is, according to the SELEN-output, 41.6 mm, or on average 0.38 mm/yr. 46

4.2.4 Same as in figure 4.2.1, but for the **IM85** ice model. The corresponding total eustatic sea level change for the period is, according to the SELEN-output, 98 mm, or on average 0.89 mm/yr. 47

4.2.5 Cross-sections of the relative sea level change rate in mm/yr for the 4 GrIS-projections along latitude 60° (blue triangles) and 75° (red crosses). The x-axis denotes the distance in km from longitude -35° W at the Greenland west coast. The RSL-change rate is on a logarithmic scale ranging from 0.1 mm/yr to 0.001 mm/yr. 48

4.3.1 Present-day GIA-induced RSL-change rate in mm/yr for ICE-5G (left) and ICE-GR (GRACE) (right). 49

4.3.2 RSL change rate in 2100 (mm/yr) for the 4 GrIS-projections. From top left: IMGRt, IMGRa, IM45 and IM85 50

5.1.1 Left: Ice discharge response to a linear increase in ocean temperature by Fuerst et al (2015)[9]. Right: Ice discharge in 2100 corresponding to a medium warming scenario by Fuerst et al (2015)[9]. 52

5.2.1 Present sea level change rates for ICE-5G(VM2) and ICE-6G(VM5a). The difference of the two ice-models is shown on the right. 54

5.2.2 Present-day GIA uplift rates computed with ICE-5G ice model with four different rheological models. Panel (a) is similar to this study. From Spada et al., 2012 55

5.2.3 RSL outputs from SELEN compared to observations, from Spada and Stocchi (2012)[28] 56

5.2.4 Comparison of Fennoscandian uplift rates interpreted along profile AB with uplift rates calculated for two different models of mantle viscosity (from Cathles (1975)). 57
5.2.5 Relative sea-level change rates from present change of ice masses. The green line indicates the ice sheet's contribution to eustatic sea level change rate (1.4 mm/yr). From Bamber and Riva (2010) 58
5.2.6 Rate of global sea level variation associated with the M3 GrIS ice model (a) (from Sørensen et al, 2011[31]). b) has the same total mass loss as M3, but with uniformly spatial melt. The white line indicates the eustatic sea level ($\approx 0.67 mm/yr$). From Spada et al., 2012[28] 59
5.2.7 Change rate of the vertical displacement (left) and the geoid (right) for the IMGRa-model. 60

List of Tables

1.2.1 Global mean sea level rise contributions in mm/yr over different time intervals from observations [5]. 9

3.1.1 The earth parameters for the 5-layer earth model (VM2) used for SELEN. 22

3.2.1 The properties of the ice-history models used in this study. . 23

3.2.2 The areas of with the possibility of ice defined in this study. 27

Contents

1 Introduction **5**

1.1 How to read this thesis 7

1.2 Eustatic sea level 7

1.3 Contributions to relative sea level changes 10

1.3.1 Glacial isostatic adjustment and sea level 12

1.3.2 Today's ice sheet melt and sea level 13

2 Theory **14**

2.1 Glacial Isostatic Adjustment 14

2.1.1 Green's Functions 16

2.2 The Sea Level Equation 17

2.3 The mass balance of ice sheets 18

3 Data and Method **21**

3.1 Earth model 21

3.2 Ice history models 22

3.2.1 Post Glacial Ice Model 24

3.2.2 Ice history from GRACE-data 25

3.3 GrIS predictions for the 21st century 28

3.3.1 GrIS MB-projections from GRACE (IMGRa, IMGRt) 28

3.3.2 SMB-projections 31

Mass balance budget predictions (IM45, IM85) 33

3.4 SELEN 36

3.4.1 SELEN-configuration 36

4 Results **37**
4.1 Long term vs short term GIA-predictions 38
4.1.1 GIA-predictions from ice changes since LGM 38
4.1.2 GIA-predictions from GRACE-observed ice melt . . . 39
4.1.3 Geoid changes and vertical uplift 39
4.1.4 ESL-change from ICE-5G and ICE-GR 41
4.2 GIA-predictions of GrIS-projections 43
4.2.1 Fingerprints from GrIS-projections 43
4.3 GrIS-GIA contribution to sea level change at Denmark's coastlines 49

5 Discussion **51**
5.1 Uncertainties connected to GrIS mass balance 52
5.2 Uncertainty of GIA-predictions 53
5.2.1 Earth parameters 53
5.2.2 Long term GIA-predictions 54
Fennoscandinavian uplift 54
SELEN reliability 55
5.2.3 Short-term predictions 55

6 Conclusions and suggestions for further studies **62**

A SELEN configuration file **70**

Chapter 1

Introduction

Changes of the Earth's sea level is one of the most severe effects related to anthropogenic climate change. The rise in lower atmospheric temperature has caused extensive melting of the ice-sheets in polar regions and other glaciers in all regions of the world (Chuch et al, 2013 [5]) and the following transformation from land-ice to ocean water has contributed significantly to a sea level rise.

The additional water is not evenly distributed to the world's oceans. Where the additional water "flows" depends on several atmospheric and geophysical processes. Regional sea level change are in magnitude often larger than the mean sea level rise (a.o. Spada et al., 2012 [28]), and is thus important to quantify, so that coastal societies are able to adapt to the changing sea level.

One of the most important effects highlighted (Spada et al., 2012 [28], Church et al., 2013 [5]) when talking about regional or relative sea level (RSL) change is the glacial isostatic adjustment (GIA), where the land-masses rebound during and after deglaciation. Today, this effect is particular significant in areas of the Northern Hemisphere that were covered with large-scale ice sheets between 26500 and 20000 years BP, reaching its maximum ice-extent 21000 years BP at what is called the last glacial maximum (LGM) (a.o. Peltier 2004 [22]). It covered most of North America and Scandinavia

in a kilometre-thick ice sheet, and lasted until 10000 years BP.

Present and future deglaciation of in particular the Greenland ice-sheet (GrIS) and resulting mass exchange between land and ocean, will not only contribute to the global mean sea level (GMSL) but also have large effects on the RSL ([1]). The GIA-effect of present day and future mass changes and it's contribution to RSL is even though less investigated, and is attempted quantified in this study.

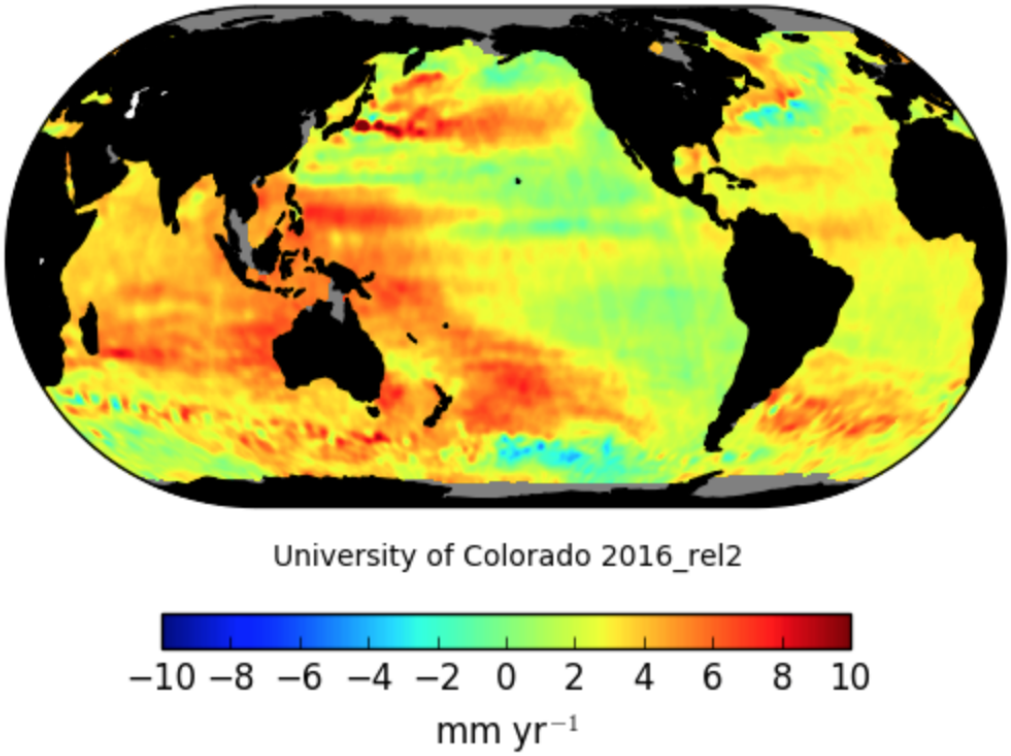

Figure 1.0.1: Local sea level trends determined for a finite period (1993 - 2016) by altimeter data. They reflect the impact of decadal scale climate variability and local sea surface height trends, which includes crustal displacements, glacial isostatic adjustment (GIA), steric effects, and even change in local wind patterns. Source: `http://sealevel.colorado.edu/content/map-sea-level-trends`

Farrel and Clark (1976) [7] quantified the effect of GIA on RSL, with the sea level equation (SLE), which later was improved by Mitrovicia and Peltier

[16] and constitutes the backbone of this study's GIA-predictions.

1.1 How to read this thesis

The reader is encouraged to read this thesis the way that suits the reader best. Every chapter is thought written in a way, that it is meaningful even without reading preceding chapters. But, in order to get the full ideas and chain of thoughts, the chronological reading order is recommended.

After a brief introduction on the general processes affecting GMSL and RSL, the next chapter will be giving a more detailed theoretical disquisition of the GIA-effect and sea level change.

The data and method section introduces the datasets and processes that underlies the production of the sea level predictions, which are presented in the result chapter, followed by a discussion of the obtained results.

1.2 Eustatic sea level

The Intergovernmental Panel of Climate Change (IPCC [5]) is using the descriptive term *global mean sea level* (GMSL) for what usually in the scientific community is called the eustatic sea level (ESL). It is defined as the mean distance from earth's centre to the ocean surface and is primarily changed by two dominant processes ([5]).

1. Thermal expansion of water
2. Mass flow from land to ocean as a consequence of melting glaciers, ice caps and ice sheets [1]

The thermal expansion is a outcome of the warming of the lower atmosphere that expands the water volume. Recent climate change has resulted in a thermal expansion corresponding to an ESL-rise of 1.1 mm/yr on average for the last two decades, according to the latest IPCC report [5] . See also table 1.2.1 for an comparison of the contributions to ESL-rise.

[1] Ice sheets are the contributions from Greenland and Antarctica

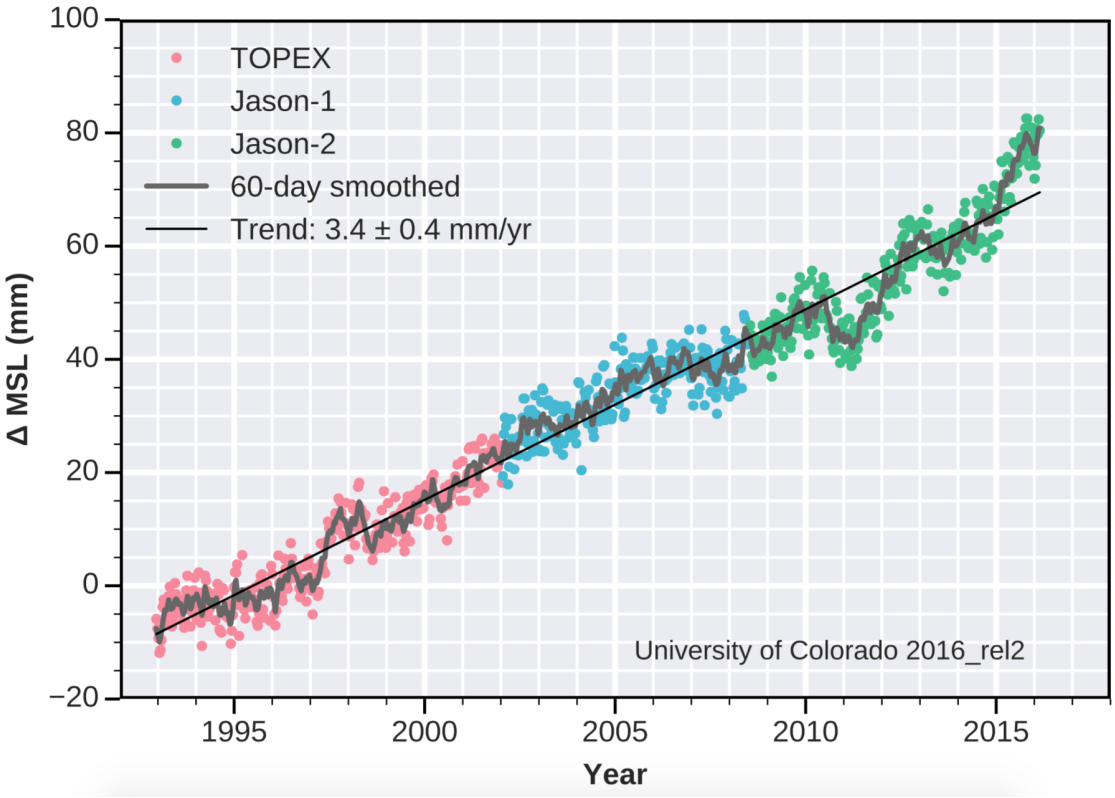

Figure 1.2.1: Global mean sea level from 1993 to 2016 as estimated from satellite altimeter data. The average trend for the period i 3.4 ±0.4 mm/yr. Taken from `sealevel.colorado.edu`

The second important driver that raises the sea level is the melting of ice that rests on solid land and flows into the worlds oceans. By far is the most ice stored in the ice sheets of Greenland and Antarctica, by storing approximately 77 % of the global surface freshwater, with Antarctica counting for the 70 % (Meier et al., 2007 [15]). A total melting of the ice sheet of Antarctica would result in a eustatic sea level rise of more than 61 meters, whereas a total melting of the Greenland ice sheet (GrIS) would be equivalent to a ESL-rise of 7 meters (IPCC 2013[5]). A total melt of glaciers and smaller ice caps[2] would only result in about 0.5 meter sea level rise, when spread evenly on the ocean surface. These numbers include effects of isostatic rebound and seawater replacing grounded ice below sea level, and is therefore less than

[2]an ice sheet is defined as an ice cap that is greater than 50,000 square km.

Source	1993-2010	5% − 95% confidence interval
Thermal expansion	1.1	[0.8 − 1.4]
Glaciers w/o Greenland & Antarctica	0.76	[0.39 − 1.13]
Greenland ice sheet & glaciers	0.43	[0.32 − 0.53]
Antarctic ice sheet	0.27	[0.16 − 0.3]
Land water storage	0.38	[0.26 − 0.49]
Total of contributions	2.8	[2.3 − 3.4]
Observed GMSL rise	3.2	[2.8 − 3.6]

Table 1.2.1: Global mean sea level rise contributions in mm/yr over different time intervals from observations [5].

the sea level equivalent of the ice volume (IPCC 2007 [13]).

Between 1993-2010 Church and White[6] estimated a GMSL rise of 3.2 ± 0.4 mm/yr from the satellite data and 2.8 ± 0.8 mm/yr from in situ data (Church and White, 2011[6]). With updated altimeter-data, the University of Colorado estimates the updated trend from 1993-2016 to be 3.4 ±0.4 mm/yr (see figure 1.2.1).

In general the sea level equivalent of any melting ice S^E can be calculated as

$$S^E = -\frac{m_i(t)}{\rho_w A_O}, \tag{1.1}$$

where m_i is the mass of the melting land-based ice, ρ_w is the density of ocean water (approximately 1026 kg m^{-3}) and A_O is the oceanic area (approximately $3.62 \times 10^8 km^2$). Simplified would a mass-loss of 100 Gt ice be equivalent to about 0.28 mm ESL rise. S^E is also called the glacio-eustatic sea level change. In context of SLE it is defined as the eustatic sea level change, since other effects are neglected in SLE.

Another significant contributor to current ESL rise, but not in particular highlighted, is last decades decay of land water storage in some areas. The water storage is highly variable on annual and decadal time-scales, and there

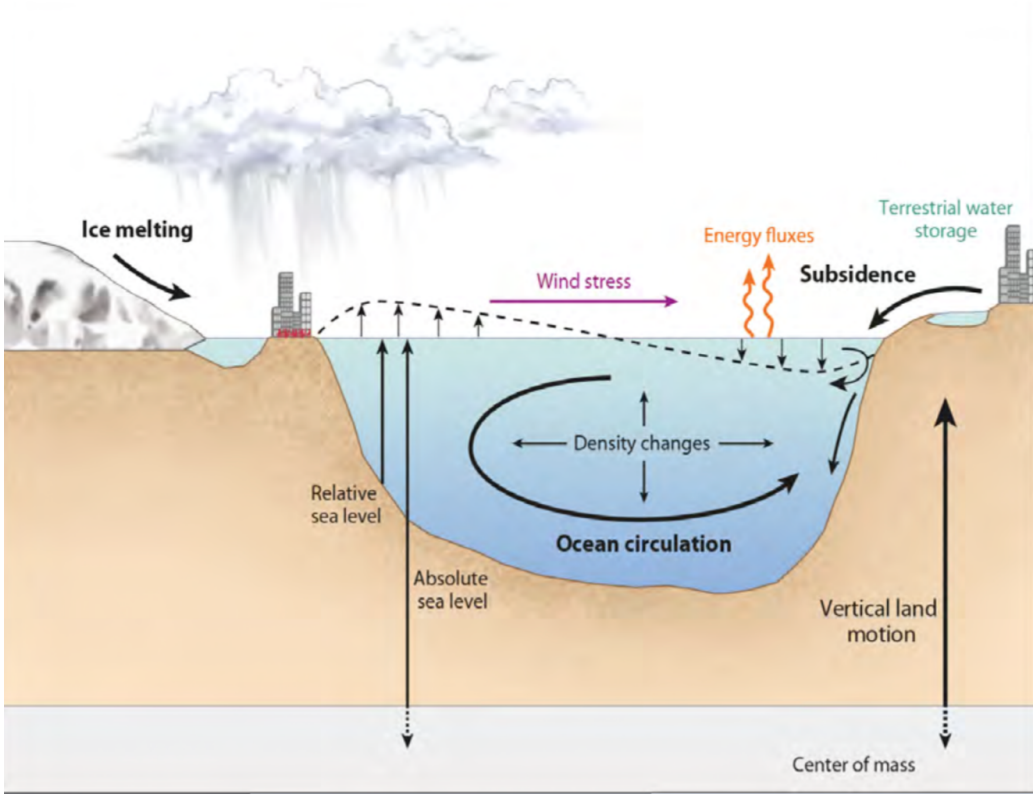

Figure 1.2.2: Processes affecting relative and eustatic sea-level. World Climate Research Programme, 2011.

is no proven long-term change in the amount of water stored on land compared to that stored in oceans (IPCC 2013[5]). The contributions during the last two decades can to some extent be explained by significant El Niño Southern Oscillation (ENSO) events during this period, where the precipitation over oceanic areas usually increases and land precipitation decreases in the tropics (Cazenave et al., 2012 [3]).

1.3 Contributions to relative sea level changes

Relative sea level (RSL) is the distance from the ocean bottom to the sea surface. Changes in RSL are substantially different from the eustatic sea level, and can in some regions be magnitudes larger than the ESL-changes.

The dynamics influencing RSL can have natural causes or be influenced by anthropogenic changes. The time scales of the involved processes can vary from being inter daily to ten thousands of years, so when looking at RSL-changes the time scale is essential [1].

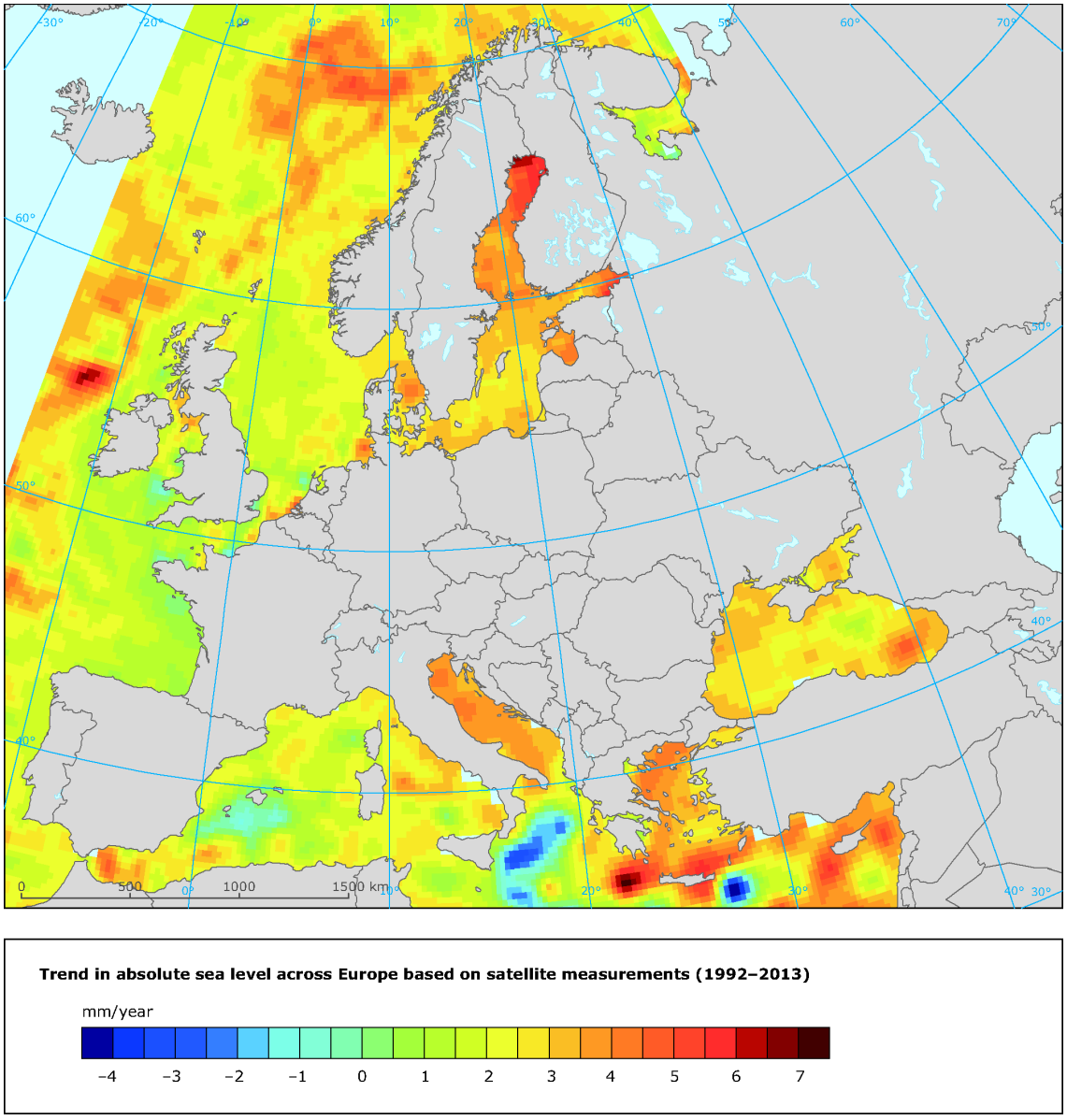

Figure 1.3.1: Local sea level trends determined for a finite period (1992 - 2013) by altimeter data. Source: `http://sealevel.colorado.edu/content/map-sea-level-trends`

Other effects that change the RSL are foremost steric effects, which refers to regional density changes due to variability in temperature and salinity. Secondly, long-lived changes in ocean circulation[5], changes in wind patterns and long-term change of the tidal cycles, caused by changes in the gravitational attraction by the moon and sun play minor roles, when discussing RSL [5]. A map of the current local RSL-trends is shown in figure 1.0.1.

1.3.1 Glacial isostatic adjustment and sea level

The GIA-effect covers changes of the geoid and vertical movement of the lithosphere, which both contributes to sea level changes. Since LGM coastlines are uplifting and ocean bottoms are subsiding, as a consequence of the retreat of the huge ice masses. This is causing large regional sea level changes, and averaged over the global ocean surface, the GIA-contribution to the sea level change (ESL-change) is estimated to be -0.3 mm/yr (Peltier, 2001, 2002, 2009; Peltier and Luthcke, 2009). The main relative sea level changes are happening in and around Scandinavia and North America, with sea level change rates in the order of centimetres per year as a consequence of GIA.

1.3.2 Today's ice sheet melt and sea level

In the context of recent change of ice sheets and glaciers, the major long term processes affecting the relative sea level are gravitational and Earth rotational effects (Bamber and Riva (2010), shown in figure 1.3.2). The GIA-effect of the current melt is often neglected, due to the short time-scale.

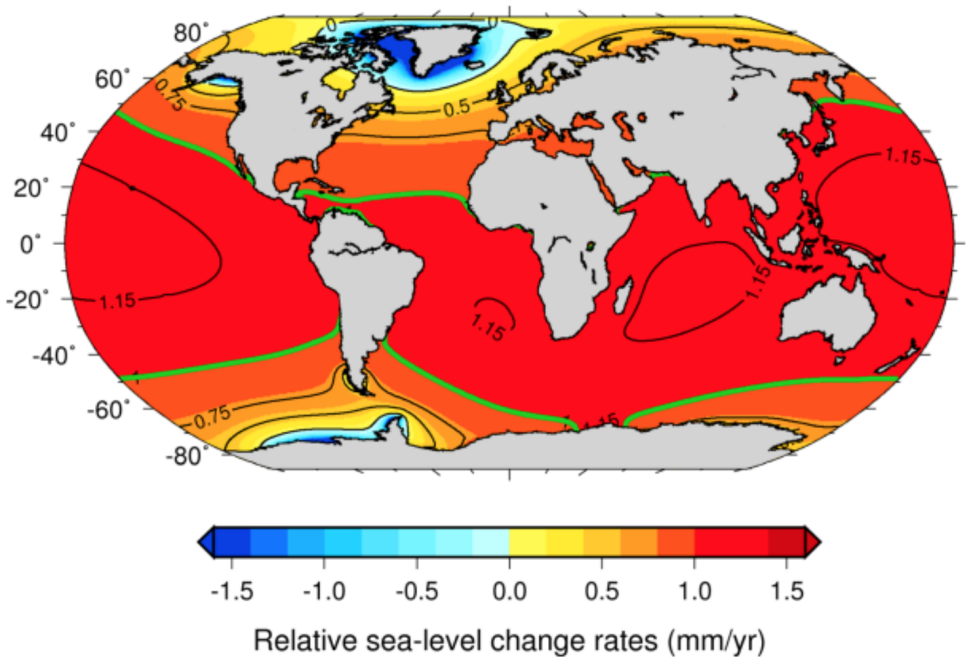

Figure 1.3.2: Relative sea-level change rates from present change of ice masses. The green line indicates the ice sheet's contribution to eustatic sea level change rate (1.4 mm/yr). From Bamber and Riva (2010)

The motivation of this thesis is to quantify the GIA-contribution to RSL of current and future ice melt of in particular the Greenland ice sheet, and hence map it's importance for sea level investigations.

Chapter 2

Theory

The sea level varies as a consequence of geophysical dynamics and thermodynamics. The variations can have well defined cyclic periods, like the gravitational effects from the sun and moon, or be rather chaotic as it depends on meteorological dynamics, like atmospheric pressure and temperature. Many of these dynamics changes the sea level immediately, while others like the viscoelastic rebound since the last glacial maximum (LGM) 21 kyr's ago is still effecting parts of the Northern Hemisphere.

2.1 Glacial Isostatic Adjustment

The patterns in the sea level caused by GIA are called 'sea level fingerprints' (a.o. Mitrovica et al., 2001[17]). It is described by the Green's Functions, that are able to quantify the three-dimensional displacement and the variation of the gravitational potential when a point-like impulsive load is applied to the surface of a symmetrically, layered model of the Earth (Spada and Stocchi (2006) [26]).

In its basic, the GIA-theory describes the response of the solid earth during glaciation and de-glaciation. When mass is gained on the surface, the crust is suppressed and the material from the viscous mantle is moved away. When the ice-load melts and after deglaciation, the layers of the Earth seek the

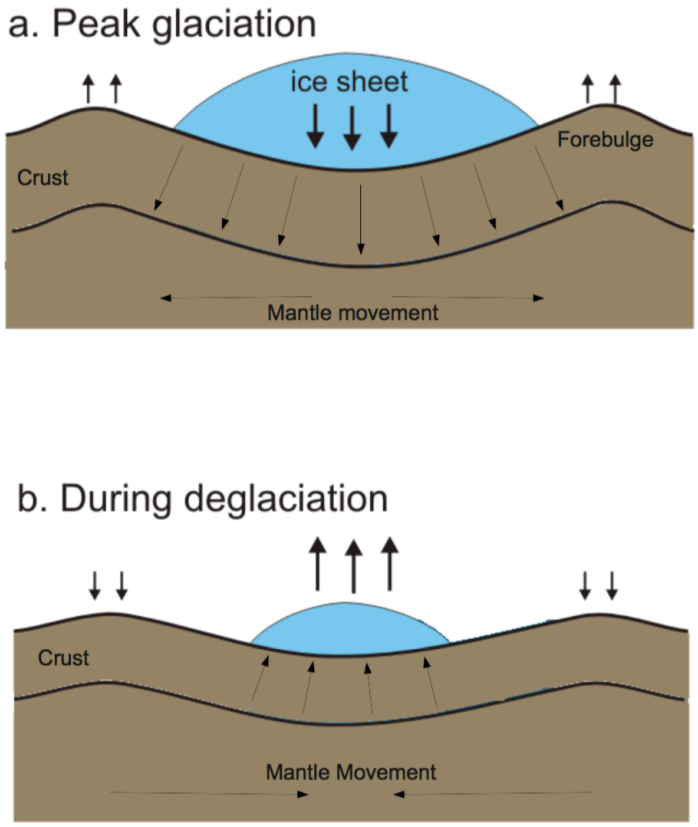

Figure 2.1.1: The solid Earth's response during peak glaciation and deglaciation. From: `gsc.nrcan.gc.ca/geodyn/images/`

state of equilibrium (figure 2.3.1), thus the crust is uplifted and the mantle regains its position. Thereby is mantle material moved towards the centre of the earlier load. At a coastline, this results in material from under the oceans is moved into land, causing a rise of the land areas and subsidence of the ocean bottoms.

The size of the load determines the depth of deformation, where a small load only affect the upper layer, can a larger load of several 100 kilometres affect deeper areas beneath the lithosphere. This is important, since the deformation behaviour of deeper layers of the earth is different from the crust, which is elastic and thus reacts immediately to a changing load.

2.1.1 Green's Functions

A point-mass load will cause a three-dimensional displacement and change the gravitational potential. The effect can be split into three scenarios. One case, where the earth is rigid, one case where the earth is elastic and thirdly one case where the earth is viscoelastic layered. Whereas the effects on the rigid earth and elastic earth responses immediately to changing mass-loads, has the viscoelastic deformation a delayed response. The sea-level Greens Functions, G_S, is a combination of the all three. It represents the offset between the Earth's geoid and the topography (Spada and Stocchi, 2006 [26]) and is defined in point P as,

$$\frac{G_s}{\gamma}(\alpha, t) = \frac{G_\phi}{\gamma} - G_u \tag{2.1}$$

Introducing the term for the surface gravity acceleration, $\gamma = GM_e/a^2$, where M_e is the mass of the Earth, a is the radius of the Earth, and G the gravitational constant. α is the co-latitude of the point P, with respect to the location of the point mass. G_u is the GF for vertical displacement, and G_ϕ is the GF for the incremental gravitational potential. In terms of the rigid, elastic and viscoelastic components, G_s gets

$$\frac{G_s}{\gamma}(\alpha, t) = \frac{G^r_\phi}{\gamma} + \left(\frac{G^e_\phi}{\gamma} - G^e_u\right) + \left(\frac{G^v_\phi}{\gamma} - G^v_u\right), \tag{2.2}$$

where the subscript, r, e, v denotes the GF's for the rigid, elastic and viscoelastic earth. G_u and G_ϕ are defined by

$$\begin{Bmatrix} \frac{1}{\gamma} G_\phi \\ G_u \end{Bmatrix} (\alpha, t) = \frac{a}{M_e} \sum_{l=0}^{\infty} \begin{Bmatrix} k_l \\ h_l \end{Bmatrix} (t) P_1(\cos\alpha), \tag{2.3}$$

k_l and h_l are called the load deformation coefficients (LDC's) or Love numbers, which are dimensionless parameters for the rigidity of a planetary body, and are defined for both the rigid, elastic and viscoelastic earth. $P_1(\cos\alpha)$ is the Legendre polynomial of degree l.

2.2 The Sea Level Equation

The Greens Functions are essential for solving the Sea Level Equation (SLE), that can determine the sea level variations that are associated with the glacial isostatic adjustment (GIA). It follows the theory of Farrell and Clark (1976), and describes variations of relative sea level due to ice-load changes. The sea level change, S is defined as the offset between the geoid height change, N and the vertical displacement, U.

$$S(\omega, t) = N - U \tag{2.4}$$

$$N(\omega, t) = r'_g - r_g \tag{2.5}$$

$$U(\omega, t) = r'_s - r_s, \tag{2.6}$$

where r'_g is the distance from the centre of earth to the geoid, r'_s is the distance of the solid surface of the earth. r_g and r_s denotes the value at a remote time t_0 and ω represents the spatial coordinates. Since N and U is defined on the whole sphere of the Earth, a reduced SLE is introduced

$$Z(\omega, t) = OS \tag{2.7}$$

Here is O the ocean function (OF), that is defined by being 1 over the surface of the oceans, and 0 everywhere else. Using the Greens Functions, in the version by Spada and Stocchi, 2006, the SLE is written as

$$S = \frac{\rho_i}{\gamma} G_s \otimes_i I + \frac{\rho_w}{\gamma} G_s \otimes_o S + S^E - \frac{\rho_i}{\gamma} \overline{G_s \otimes_i I} - \frac{\rho_w}{\gamma} \overline{G_s \otimes_o S}, \tag{2.8}$$

where S is the wanted sea level change, I is the ice load function, $\otimes_i$ and $\otimes_o$ implies spatio-temporal convolution over the surface defined by the ice history and ocean function, respectively. S^E is the glacio-eustatic sea-level change, defined in eq. 1.1. Equation 2.8 is an integral equation and thus it must be solved iteratively, fo which the open-source Fortran 90 SLE-solver, SELEN 2.9 is used.

2.3 The mass balance of ice sheets

The sea-level equation (Eq. 2.8), has the space-time evolution of the ice cover as the only physical input-parameter that is time-dependent, namely the ice function $I(\omega, t)$. The changing ice sheets are measured as the thickness of the ice, with a certain temporal and spatial resolution. Spada and Stocchi (2006)[26] define the variation of a given ice thickness, $T(\omega, t)$ at a location with coordinates, ω and at a time, t as

$$I(\omega, t) = T(\omega, t) - T_0 \tag{2.9}$$

Where T_0 is the ice thickness at the location at a reference time.

The associated mass change of the whole ice sheet is calculated as

$$m_i(t) = a^2 \int_i d\omega \rho_i I(\omega, t) \tag{2.10}$$

where, $d\omega = \sin\theta d\theta d\lambda$, with λ representing the longitudes and θ the co-latitudes. The average ice density, $\rho_i = 931$ kg m^{-3} and the radius of the earth, $a = 6371$ km. i is the region where $I(\omega, t) \neq 0$, i.e. the area where there is a variation of the ice mass.

The ice mass changes when ice evaporates, melts and runs off in the oceans (mass loss) or because of snowfall (mass accumulation). These surface changes are defining the surface mass balance (SMB) of the ice sheet. Usually, as in the case for GrIS, is the net-change positive over a calendar year, meaning there is a more accumulation than melt.

The accumulation of mass on the ice sheet, pushes the ice towards the border and consequently into the surrounding ocean, where it breaks of as sea ice, and keeps the mass-balance of the ice sheet. This effect is summarized under the term dynamic ice-loss (DIL) (van der Broecke, 2009 [2], Kjeldsen et al, 2015 [11]).

Rising atmospheric temperatures however, is changing this balance. While

global warming is believed to cause greater snowfall on the GrIS, the melting season has increased significantly, and the summer days are getting hotter, resulting in a smaller, but yet positive SMB.

The net mass balance (MB) is the sum of DIL and SMB:

$$\mathrm{MB} = \mathrm{DIL} + \mathrm{SMB} \tag{2.11}$$

for clarification, $\mathrm{DIL} < 0$ in areas where there is dynamic mass loss.

The surface mass balance is mainly a result of two meteorological effects: ice accumulation because of snowfall, and melting of ice as a result of days above 0°C. A regional climate model can be used to determine each of these effects and thus calculate SMB (Fettweis et al., 2013 [8]).

The dynamic ice loss is estimated from ice sheet dynamics, that describe the mostly gravity-driven motion by parts of the ice within an ice sheet. This motion is rather difficult to predict since the activity of ice is often happening in periodic cycles, with longer periods of inactivity (van der Broecke et al, 2009[2]).

The two driving factors to dynamic ice changes are temperature and the strength at the bases (Fuerst et al, 2015[9], Yan et al, 2014[35]). Both parts are influenced by current climate change. Thinning of ice shelfs due to melting glaciers, is reducing the stability of the ice. Furthermore it has been reported that melt-water can permeate through the ice to bases of the ice, where it can act as a lubricant and speed up the ice-dynamics (Yan et al, 2014[35]).

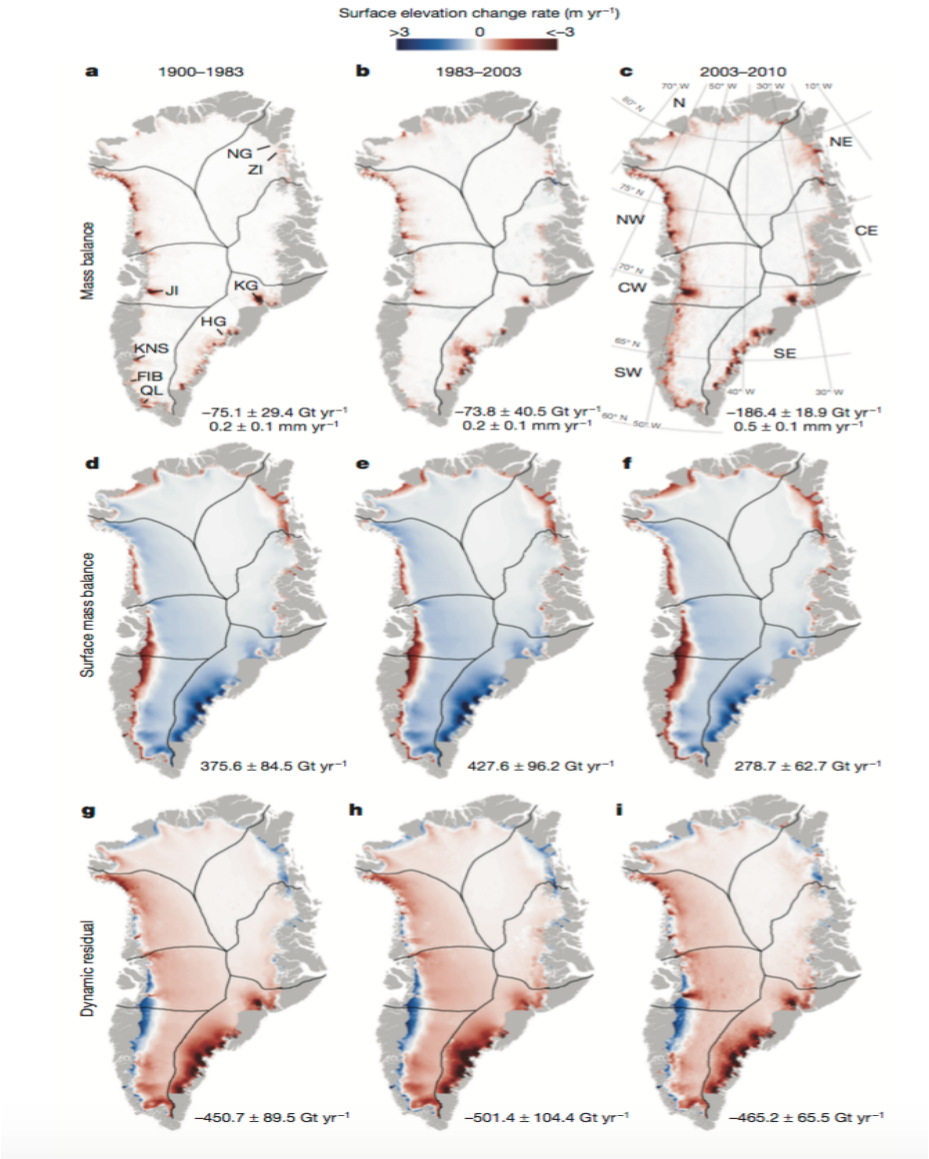

Figure 2.3.1: Surface elevation change and mass balance of GrIS. The total MB, SMB and DIL is shown for the periods 1900-1983 (left), 1983-2003 (middle) and 2003-2010 (right). From Kjeldsen et al (2015)[11].

Chapter 3

Data and Method

For the sea level equation and GIA calculations mainly two things are required: An earth model with a rheological profile and an ice model providing a glaciation chronology for the ice sheet(s) of which the GIA-effect is investigated.

3.1 Earth model

As a part of the code for SELEN (that solves the SLE), a Fortran post-glacial rebound calculator called TABOO, determines the load deformation coefficients (LDC's) from an specified rheological profile (see table 3.1.1). In the model it is assumed that the Earth has a spherical geometry and acts as an incompressible Maxwell body, with an elastic lithosphere followed by layers with viscoelastic behaviour, which all respond and deforms to the changing ice load at the Earth's surface.

For all analysis made in this report the earth layer profile is kept at the default setting set by Spada (2006) [26]. The earth parameters are shown in table 3.1.1.

Layer	Depth range [km]	Density [kg/m^{-3}]	Shear modulus [GPa]	Viscosity [10^{21} Pa·s]	Gravity [m·s^{-2}]
Lithosphere	$0-110$	4120	73	∞	9.707
Shallow upper mantle	$110-420$	4120	95	0.5	9.672
Transition zone	$420-670$	4220	110	0.5	9.571
Lower mantle	$670-2891$	4508	200	2.7	9.505
Core	$2891-6371$	10925	0	0	10.622

Table 3.1.1: The earth parameters for the 5-layer earth model (VM2) used for SELEN.

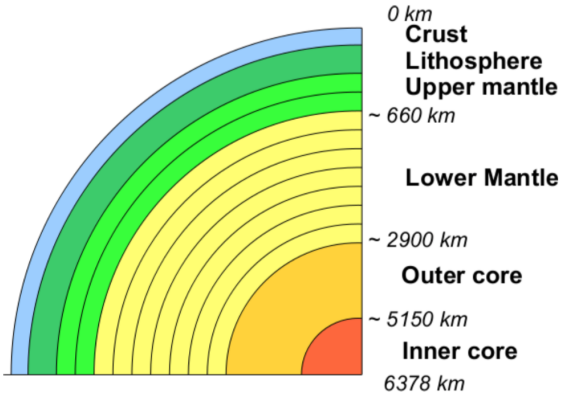

Figure 3.1.1: A simplified spherical earth model. Denotions of depth-range do not necessarily align with the depth range used in the VM2-model and their size is not in-scale. From Sørensen et al. (2010).

3.2 Ice history models

The second input needed for the GIA calculations are ice sheet histories, that describe the change of glaciation during a period of time. The ice histories used in this study is spanning different time periods (see table 3.2.1).

The software package for SELEN includes the ice model ICE-5G by Peltier (2004) [22]) with a glaciation chronology from the last glacial maximum (LGM) to present.

A present day global ice history, ICE-GR, is obtained from GRACE-observations

from 2003-2014, which allows us to compare long-term with short-term GIA-predictions.

Besides the global, historic ice-histories, four different projections for the future deglaciation of GrIS is made:

1. **IMGRa:** Mass balance (MB) trends from GRACE-observations (2002-2014) for GrIS is combined with MB-accelerations, and projected from 1990-2100.

2. **IMGRt:** An enforced mass balance (MB) trend from GRACE-observations (2002-2014) is projected.

3. **IM45:** Surface mass balance (SMB) projections in a RCP4.5-scenario from the EC-Earth climate model and GRACE-observations is used to estimate the dynamic ice loss (DIL). For the IM45-model the DIL is kept at a constant level.

4. **IM85:** Same as IM45 for a RCP8.5-scenario environment. The DIL is accelerated (see figure 3.3.1).

For the overview, parameters of each model is shown in table 3.2.1.

Ice-history model	Time span	Spatial resolution	Temporal resolution	Ice sheets	ESL change [mm/yr]
ICE-5G	21 kyr - present	1x1°	1000 yr	Global	5.8
ICE-GR	2003-2014	1x1°	1 yr	Global[1]	0.62
IMGRa	1990-2100	1x1°	10 yr	GrIS	0.93
IMGRt	1990-2100	1x1°	10 yr	GrIS	1.01
IM45	1990-2100	1x1°	10 yr	GrIS	0.38
IM85	1990-2100	1x1°	10 yr	GrIS	0.89

Table 3.2.1: The properties of the ice-history models used in this study.

The 4 different MB-projections of the GrIS are compared in figure 3.3.1. It is seen that IMGRt, IMGRa and IM85 has about same mass loss history, whether the IM45-history remains at the same level as the GRACE-

[1]selected areas with ice-cover. See table 3.2.2.

observations. This is interesting, since it makes it possible to compare different spacial melt histories of GrIS, that in total gives the same eustatic sea level rise, but possibly have different GIA-effects.

3.2.1 Post Glacial Ice Model

The ICE-5G (Peltier, 2004) is a common ice history model used for GIA calculations. It reconstructs the ice sheet history since LGM (21 kyr ago) by combining borehole observations, relative sea level (RSL) observations and modelled RSL-data.

The model-setting used in SELEN, has 22 time-steps, spanning from 21 kyr ago at LGM to present, giving a temporal resolution of 1000 years. It comes in a 1x1° spatial resolution. The total elevation change from the deglaciation of the northern hemisphere is visible in figure 3.2.1.

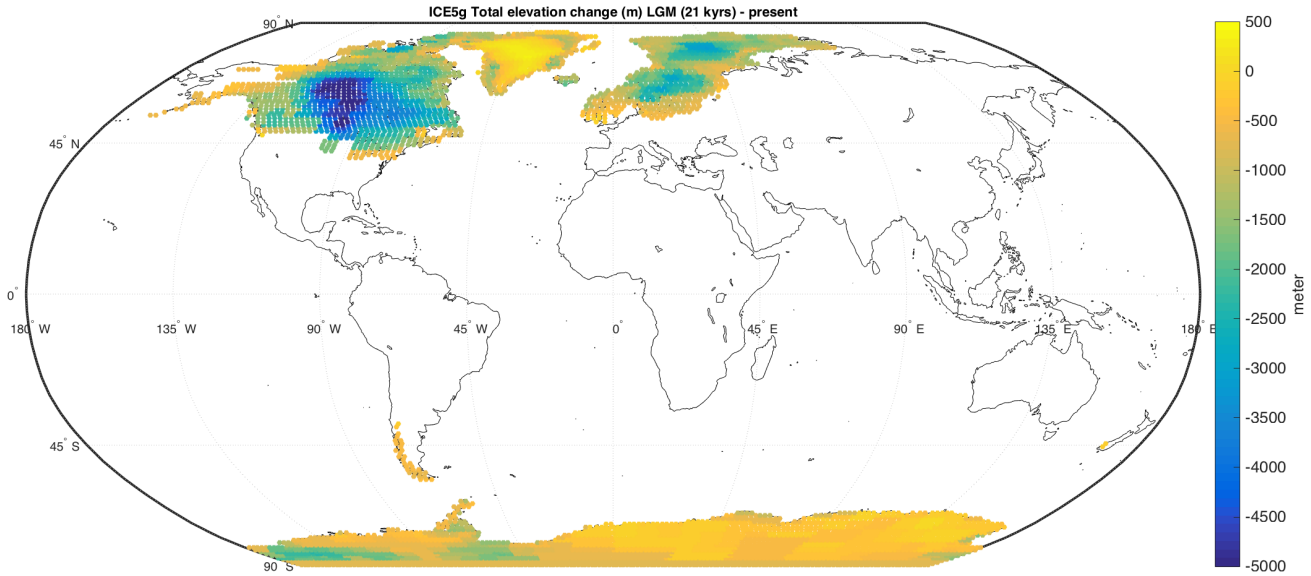

Figure 3.2.1: ICE-5G total elevation change from 21 kyr to present.

3.2.2 Ice history from GRACE-data

The Gravity Recovery and Climate Experience (GRACE) was launched by NASA and the German Space Agency (DLR) in March, 2002. It consists of a set of twin-satellites measuring the gravity-field of the earth from two identical orbits, separated by around 220 km. By using microwaves the satellites are monitoring the distance between them very accurately, which varies slightly when passing the spatial gradients of the earth's gravity field. By recording those variations, the gravity field of the earth can be mapped.

The satellites signal is on ground transformed into physical quantities like satellite-to-satellite distance. To process these so-called level 1 data to physical quantities, spherical harmonics are used to obtain a set of gravity field solutions, which is thoroughly described by Wahr et al. 1998 and Wahr et al. 2007. The gravity field is transformed into a measure of mass variations, i.e. equivalent water heights (EWH). The third release of the time variable models from GRACE from the french Space Geodesy Research Group (GRGS, available at: `http://grgs.obs-mip.fr/grace`), is used for the ice histories. A map of the total elevation change measured by the GRACE-satellites for the ice sheets of the world is shown in figure 3.2.3.

The solutions are provided in a temporal monthly resolution spanning from April 2002 to March 2015 and given in EWH and as the difference to a static reference field, which is closely equal to the EWH-grid in January 2008.

The GRACE-data is cleaned from gravitational periodic variations such as Earth tides and ocean tides, thereby only differ from the reference field by effects that are not modelled, like surface mass changes from ice melting, hydrology and post-glacial rebounds. According to GRGS the data has been stabilized and hence no smoothing is necessary.

The EWH-grid is given in the spatial resolution of a 1°x 1°, starting from longitude -179.5° to 179.5° and -89.5° to 89.5°, giving a spatial field of 360 longitudes and 180 latitudes, summing up to a total grid of 64800 grid points.

The release has eight monthly solutions missing, namely the months 2003/06,

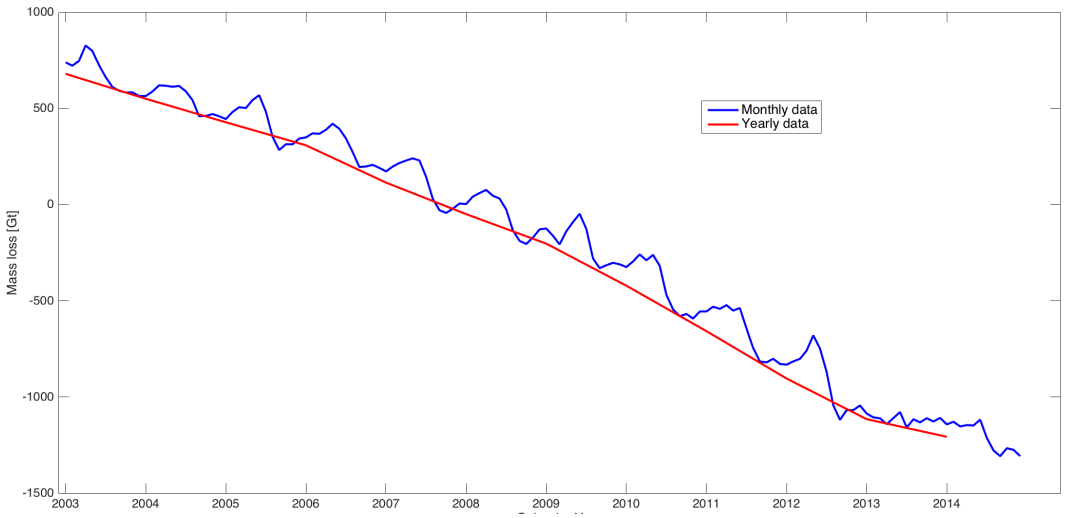

Figure 3.2.2: Monthly and yearly mass-loss obtained from GRACE-observations for GrIS relative to 2008. The average mass loss is 206 ± 68 Gt/yr. The yearly mass loss is obtained by the Jan-to-Jan difference.

2011/01, 2012/10, 2013/03, 2013/08, 2013/09, 2014/07, 2014/12. For those months the gravity field has been linear interpolated, which basically is the mean of the two neighbouring months.

The monthly EWH-data is modified to a year-by-year relative change, by taking the January-to-January difference:

$$\overline{EWH}_{yr} = EWH_{01,yr} - EWH_{01,yr-1} \tag{3.1}$$

$\overline{EWH}_{yr}$ is the yearly change of EWH. This is translated into an corresponding ice-thickness, $I(t, \omega)$,

$$I(t, \omega_i) = \overline{EWH}_{yr,i} \cdot \frac{\rho_w}{\rho_i} \tag{3.2}$$

i denotes that I is only calculated in areas with possibility of land-ice.

Practical ω_i is obtained by taking the sum of the opposite ocean function (1

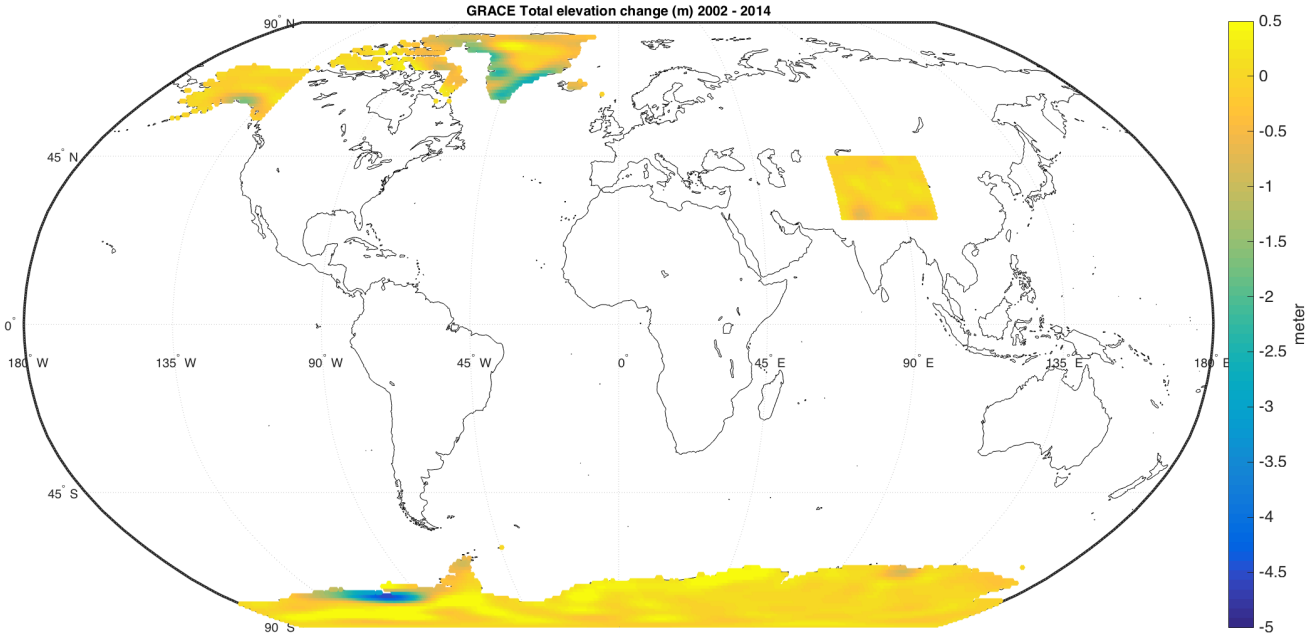

Figure 3.2.3: Total elevation change from 2003-2014 of the ICE-GR model, obtained by GRACE-measurements.

when land, 0 when ocean) in the 5 predefined ice-areas (see table 3.2.2).

$$\omega_i = (1 - O)(\omega_{\mathtt{GR}} + \omega_{\mathtt{AA}} + \omega_{\mathtt{AL}} + \omega_{\mathtt{AN}} + \omega_{\mathtt{HI}}), \tag{3.3}$$

and thus there will be areas with no ice, but the gravity variation in those areas are insignificant compared to the change in glaciers and ice sheets.

Region	Abbreviation	Longitude	Latitude
Greenland	GR	290° - 360°	60° - 82°
Arctic Archipelago	AA	230° - 290°	70° - 82°
Alaska	AL	190° - 230°	55° - 82°
Antarctica	AN	0° - 360°	-90° - -60°
Himalaya	HI	70° - 100°	28° - 45°

Table 3.2.2: The areas of with the possibility of ice defined in this study.

3.3 GrIS predictions for the 21st century

There are several methods on how to make predictions of GrIS (Sørensen et al., 2010[30]). Satellite missions during the last decade, such as GRACE, Interferometric Synthetic Aperture Radar (InSAR), ICESat (Ice, cloud and land Elevation Satellite), ERS (European Remote Sensing satellite) and Envisat have measured and monitored the ice sheet and its dynamics. The data provides information on change in gravity (from GRACE), change in elevation (from laser altimeters), accumulation data (mostly from ice-cores) and information about ice discharge and glacier movements (from InSAR).

For all methods and future scenarios the general perception that GrIS is undergoing dramatic changes and that the total ice-mass is decreasing (Sørensen et al., 2010[30]).

The mass loss estimates for the 4 different projections used in this study are shown in figure 3.3.1. As mentioned, can the mass loss be translated directly into a eustatic sea level change (100 Gt equals about 0.28 mm global sea level rise).

3.3.1 GrIS MB-projections from GRACE (IMGRa, IMGRt)

Two of the GrIS-projections are GRACE-observations projected for the 21st century. Between 2003 and 2014 the MB derived from GRACE is a mass loss of 206 ± 68 Gt/yr. But the melt is not evenly distributed, and at some locations, the ice sheet is gaining mass (see figure 3.3.2). Except of an area in north-west Greenland, the mass of the ice-sheet is decreasing. This is in particular visible along the south-east and the west-coast, where many of Greenlands significant glaciers are pulling back. The trend in height change is up to 30 cm per year.

The acceleration of the mass-change from 2003 to 2014, is shown on the right map of figure 3.3.2. This second-order effect has a different pattern than the linear trend shown and shows that the south-east is experiencing

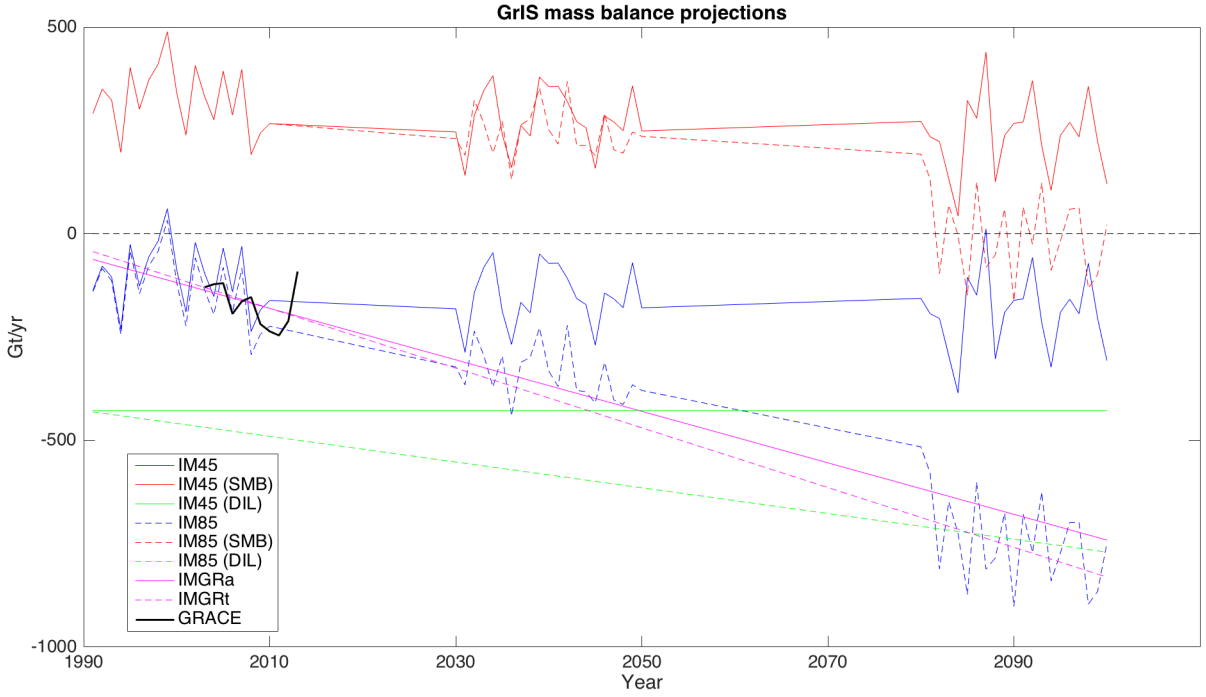

Figure 3.3.1: The yearly GrIS mass loss of the 4 projections as well as for SMB and DIL for IM45 and IM85. The original GRACE observations (from 2003 to 2014) of GrIS.

a decreasing melt, while the area north of Nuuk has an accelerating melt of the icesheet.

The **IMGRt**-ice projection, is based on the trend of the MB from GRACE-observations. Since it is the general believe that mass loss will increase ([8]), the trend has been reinforced, so that in the end of 21st century, the mass loss will be 4 times larger than today (see figure 3.3.1). On average the yearly mass-loss is 437 Gt.

For **IMGRa** the acceleration is extrapolated and added to the trend, giving an average mass-loss of 402 Gt.

The GRACE-projections are not coupled to future projections of the atmospheric temperature-trend or other modelled climate parameters. Therefore the projections are only "what-happens-if"-scenarios, and not physical

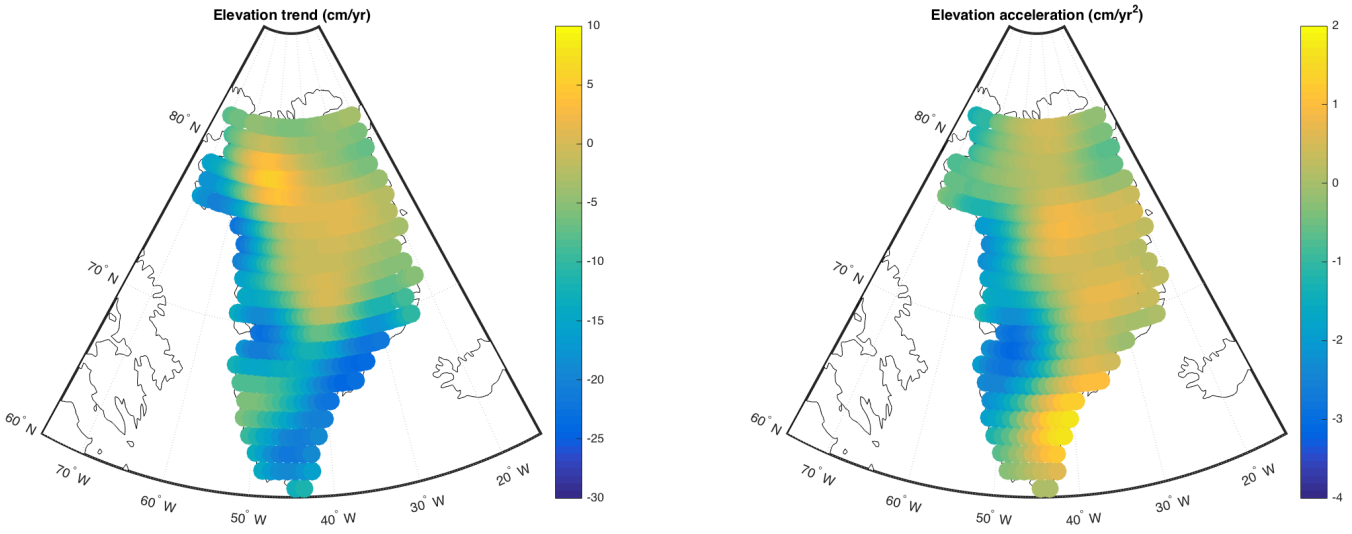

Figure 3.3.2: Trend and acceleration from GRACE-data between 2003-2014 for GrIS.

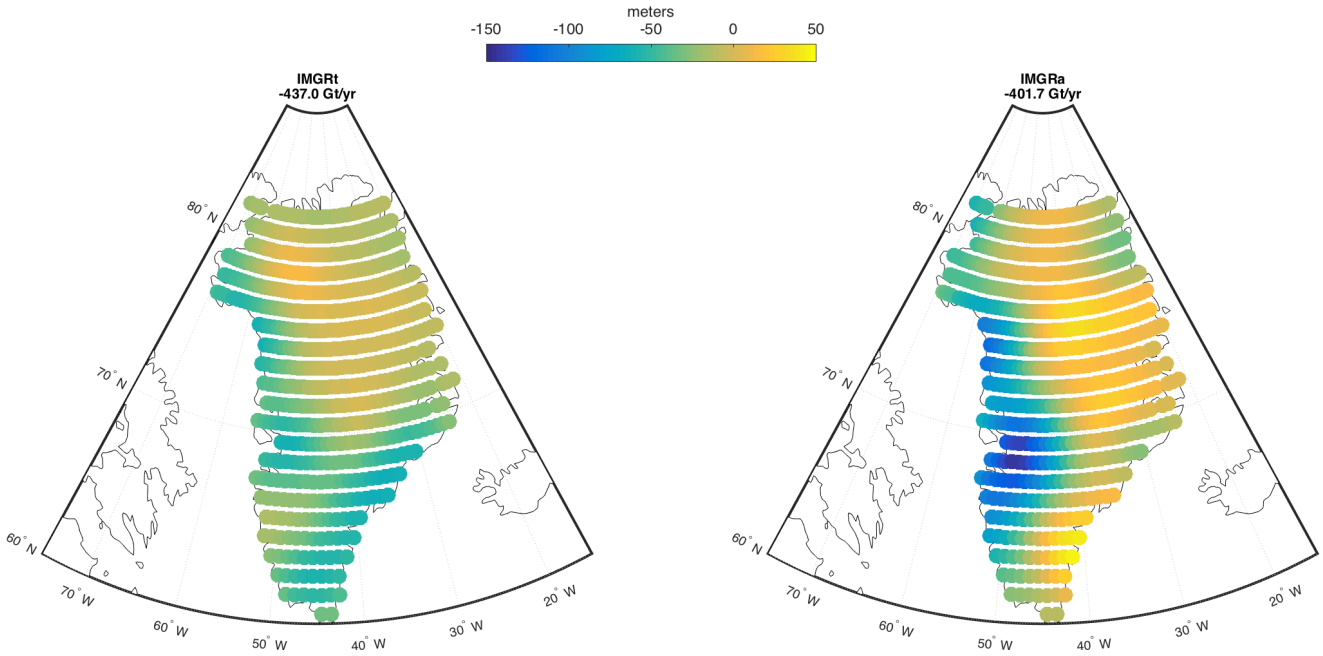

Figure 3.3.3: Projected elevation change (water equivalent) for Greenland in 2100. Left for IMGRt and right for IMGRa.

grounded visions of the future of GrIS.

3.3.2 SMB-projections

Unlike the GRACE-projections, the IM45 and IM85 ice histories for GrIS includes projections of the surface mass balance, that is coupled to a scenario of radiative forcing, the so-called Representative Concentration Pathways (RCP's) defined in the fifth IPCC report[5].

The SMB-projections is drawn from the HIRHAM regional climate model, developed by the Danish Meteorological Institute (DMI) and Alfred Wegener Institute (P. L. Langen, DMI, personal communication, 2016). It uses the boundary conditions of the EC-EARTH global climate model forced with two different RCP-scenarios, RCP4.5 and RCP8.5, representing an additional radiative forcing of 4.5 and 8.5 w/m^2 by 2100, compared to pre-industrial levels.

The two RCP-scenario-projections for the GrIS SMB is given in two 20-year periods, 2031-2050 and 2081-2100. Furthermore modelled SMB-data from 1991-2010 has been provided, in order to compare the modelled SMB to observed mass balance in last decades, measured with GRACE.

The HIRHAM SMB-data is gridded in a 300x441 matrix, covering the most of Greenland, which approximately corresponds to an average cell-size of 5x5 km. The surface mass balance in the 2 time periods is shown for each scenario in figure 3.3.4.

For use in SLE, the ice model used as input must be in a continuous equal-spaced temporal resolution. With that in mind, a interpolation is made for the intermediate periods between 2011-2030 and 2051-2080.

With b_0 denoting mean SMB between 1991-2010, b_1 for 2031-2050 and b_2 for 2081-2100, and a_0, a_1 and a_2 denoting the corresponding acceleration

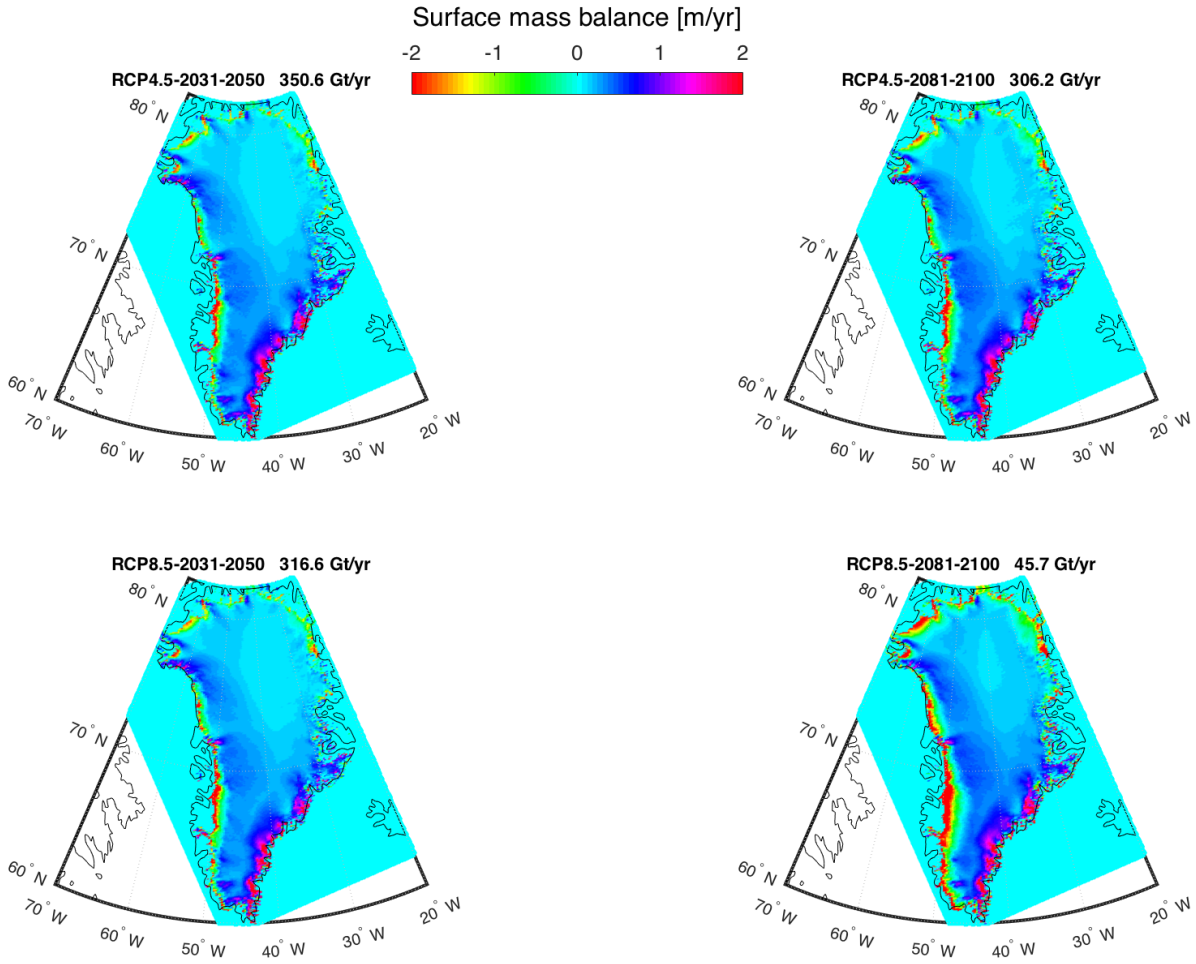

Figure 3.3.4: Average SMB trends from raw data for the RCP4.5 (top) and RCP8.5 (bottom), for the period 2031-2050 (left) and 2081-2100 (right) and their corresponding average mass change (mass gain).

[m/yr^2] of SMB, the period 2011-2030 has been calculated as

$$\mathrm{SMB}(y1, i) = \frac{1}{2}(b_{0i} + b_{1i}) + \frac{1}{2}(a_{0i} + a_{1i}) \cdot (y1 - 2010) \tag{3.4}$$

Where $y1$ is a year between 2011 and 2030 and i is a single grid-point. The next intermediate period, where $y2$ denotes a year between 2051 and 2080

is calculated in a similar way:

$$\mathrm{SMB}(y2, i) = \frac{1}{2}(b_{1i} + b_{2i}) + \frac{1}{2}(a_{1i} + a_{2i}) \cdot (y2 - 2050) \tag{3.5}$$

Mass balance budget predictions (IM45, IM85)

SMB differs from the mass balance in the way, that the ice discharge or dynamic ice loss (DIL) is not considered in SMB. In theory, the difference between SMB and the mass balance obtained by GRACE is defined by the DIL (a.o. Church et al. [5]).

Therefore the present day dynamic ice loss is estimated by using the modelled Hirham SMB-data and compare them to the GRACE observations described previously. In order to compare the GRACE 1x1-degree grid with the SMB-data, we use the MATLAB-function `griddata` to interpolate the SMB-data with the least-square method.

The 8 year span from 2003-2010 is the only time-span where GRACE and SMB-data are overlapping, in which years the dynamic ice loss is calculated as

$$\mathrm{DIL}_{2003-2010} = \mathrm{MB}_{\mathrm{GRACE},2003-2010} - \mathrm{SMB}_{2003-2010} \tag{3.6}$$

The three quantities are in EWH-change per year and shown in figure 3.3.5.

The dynamic ice-loss feedback to climate change and how it is related to temperature rise of atmosphere and oceans is quite uncertain. There is some evidence, that the DIL will increase (more ice discharge) with warmer climate, while others say it will vary, but on average be at the same level as present (van der Broecke et al[2], 2009, Fuerst et al, 2015 [9]). For covering this uncertainty, the DIL is projected differently for IM45 and IM85:

For the **IM45** ice history, the dynamic ice loss is kept at a constant level and added to the SMB-projection for RCP4.5.

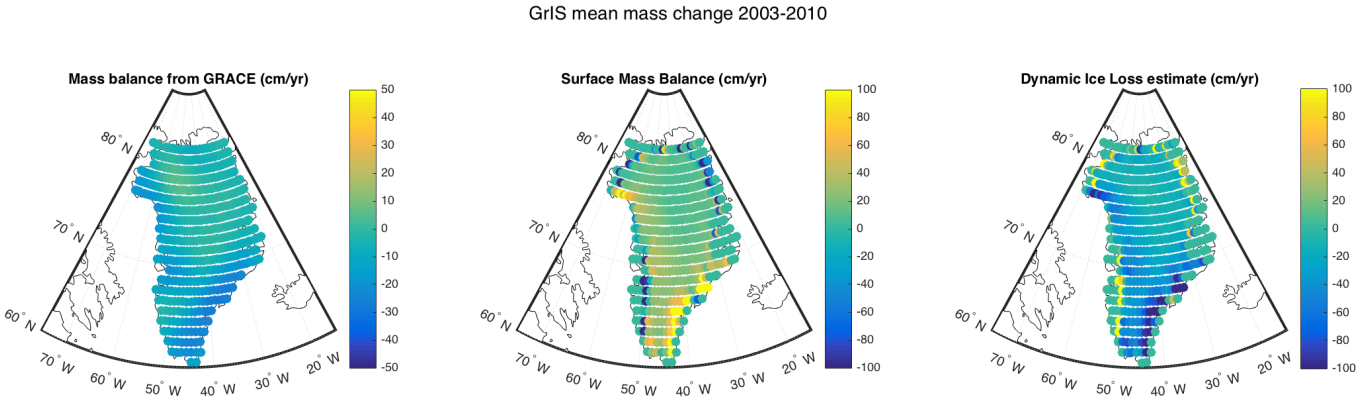

Figure 3.3.5: Average mass balance (left), surface mass balance (middle) and dynamic ice loss (right) obtained by Hirham (SMB) and GRACE (MB) for the years 2003-2010. DIL is the difference between the two.

For the **IM85** ice history, the dynamic ice loss is forced to be 80 percent larger in 2100 than in 2010 and added to the SMB-projection for RCP8.5.

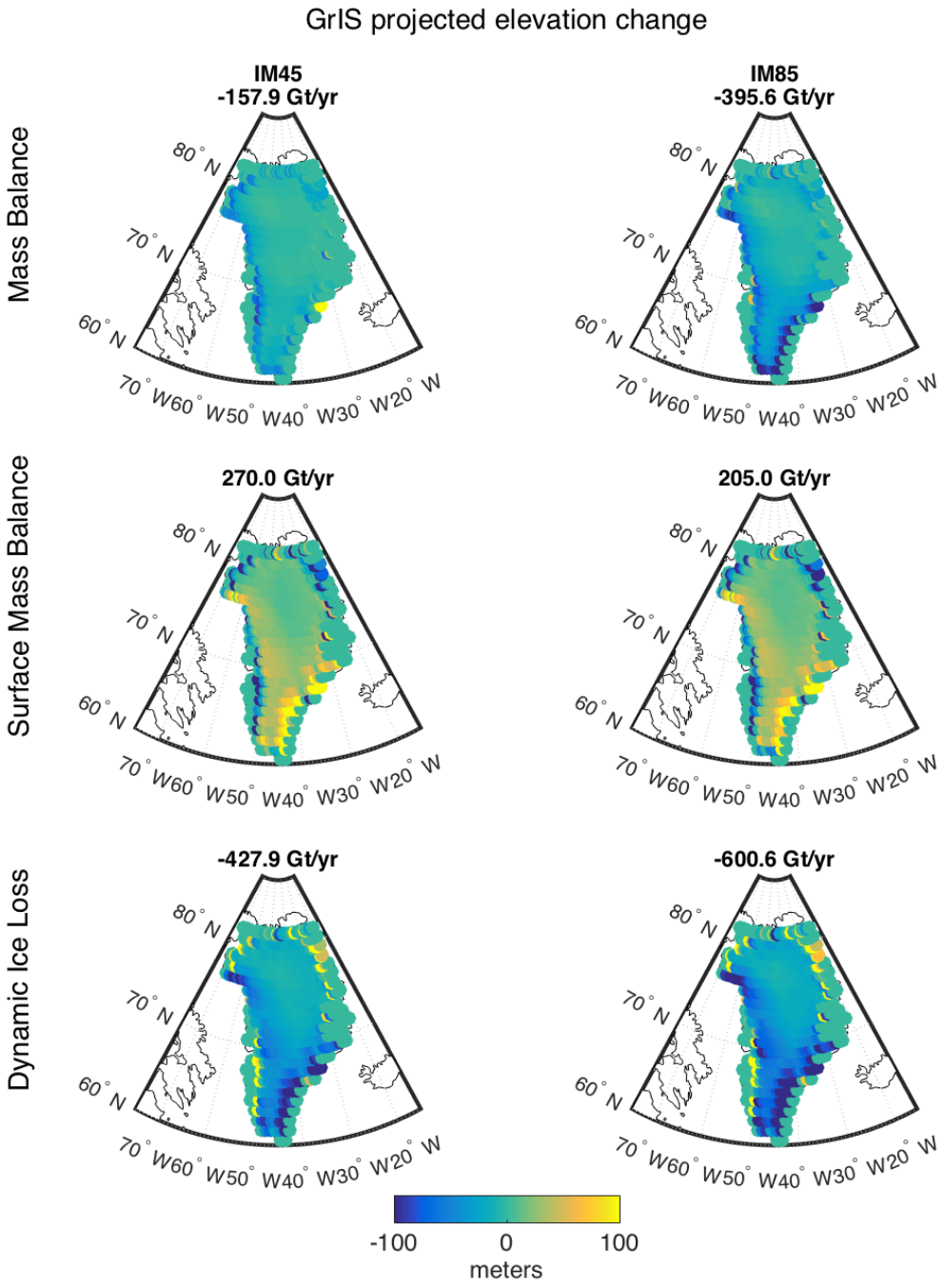

Figure 3.3.6: Mass balance (top), surface mass balance (middle) and dynamic ice loss (bottom) for ice histories of IM45 (left column) and IM85 (right column). The number above the maps, is the contribution of average mass loss from 1990 to 2100 (see also figure 3.3.1).

3.4 SELEN

SELEN is a Fortran 90 program for solving the sea level equation (SLE) numerically, developed by Computational Infrastructure for Geodynamics (CIG) and Spada and Stocchi (2006)[26]. It is maintained by an open source community. SELEN (acronym of SEa Level EquatioN solver) solves the SLE given for a uniform layered and non-rotating Earth with Maxwell viscoelastic materials.

It is an easy-to-use tool to look at the GIA-effect, given a certain glaciation history. The input file defining the glaciation history, is a set of vectors with the amount of grid points as rows. The first 4 columns sets the longitude/latitude of the grid-points with the next columns setting the ice thickness with a determined temporal distance.

3.4.1 SELEN-configuration

The input-file of SELEN looks like this:

λ`-count` λ_1 θ`-count` θ_1 $I(\lambda_1, \theta_1, t_1)$ `...` $I(\lambda_1, \theta_1, t_n)$
λ`-count` λ_2 θ`-count` θ_2 $I(\lambda_2, \theta_2, t_1)$ `...` $I(\lambda_2, \theta_2, t_n)$
...

where n is the number of time-steps and I is given in meters. Before running SELEN, the temporal distance is set (between 0.001 and 1 kyr, depending on the temporal resolution) and the ice history input-file is specified as well as an output folder in the configuration file (`config.dat`). All other configurations are remained in the default setting set by the program developers, Giorgio Spada and Paolo Stocchi ([27]).

Chapter 4

Results

The six ice history models (ICE-5G, ICE-GR, IMGRt, IMGRa, IM45, IM85, see table 3.2.1) presented in the previous chapter are used as data-input in the open source Fortran 90-program SELEN, that solves the sea level equation (SLE) for each ice model. First and foremost, it gives the change rate for the geoid and the vertical displacement at the last time-step of the ice history (i.e. for the ICE-5G model, it provides the sea level rates 21 kyr after LGM - "present-day".). The difference between the geoid and the vertical displacement defines the relative sea level (RSL) (a.o. Farrell and Clark, 1976 [7], Mitrovica and Milne, 2002) - the so-called fingerprints (Mitrovica et al. 2001 [17],; Bamber and RIva, 2010[1]). The fingerprints from SELEN only represents the changes induced by the glacial isostatic adjustment (GIA) that occurs when ice mass changes (Spada and Stocchi (2006)[26]), which does not include the immediate elastic response of the lithosphere (Spada et al., 2012[28]).

Secondly, SELEN provides the eustatic sea level (ESL) evolving over the time-span of the ice history, which can put the GIA-contributions into perspective of the total sea level changes of the changing ice sheets.

This section will present the GIA-effect of the ICE-5G ice history spanning from last glacial maximum (LGM) to present which gives an idea of the long

term GIA-processes. Similar calculations are done for ICE-GR, which is an ice-history based on GRACE-observations from 2003-2014 and thereby is on much shorter time scale.

The fingerprints from the four projections of the Greenland ice sheet (GrIS), IMGRa, IMGRt, IM45 and IM85 (from 1990 to 2100), allows us to look at the GIA-effect of the future deglaciation of GrIS. By comparing with the knowledge from the short term (ICE-GR) and long term (ICE-5G) GIA-effects, an attempt is made to quantify the size of the GIA-effect in 2100 of the region around the ice loss (Greenland) and in the region around Denmark, 2.5 thousand km away from the GrIS and hence it's relevance for future sea level adaptations.

4.1 Long term vs short term GIA-predictions

4.1.1 GIA-predictions from ice changes since LGM

The fifth generation of ice models made by Peltier (2004)[22], called ICE-5G, is a reconstruction of the surface topography and land-ice distribution since LGM 21 kyr ago, when big parts of the Northern Hemisphere were covered with ice, which in some areas were several kilometres thick (see total change in ice-thickness from LGM to present in figure 3.2.1).

Figure 4.1.1, shows fingerprints for the ICE-5G model 21 kyr after LGM (present-day). It is clearly visible, that the largest fingerprints are around the areas of ice loss, which is also shown by Peltier (2004) with the same ice history. The largest fingerprints is in the area of the Hudson Bay in Canada, with rates of -15 mm/yr, which is in agreement with similar studies of the GIA-rebound (Sella et al 2007[25]) and in-situ measurements (Spada, 2012[28]). As seen in figure 3.2.1, this is also the area of largest ice-change since LGM. In Scandinavia, the retreat of the Fennoscandinavian ice-sheet after LGM, is causing the sea level to change with up to 10 mm/yr in the northern parts of the Baltic Ocean.

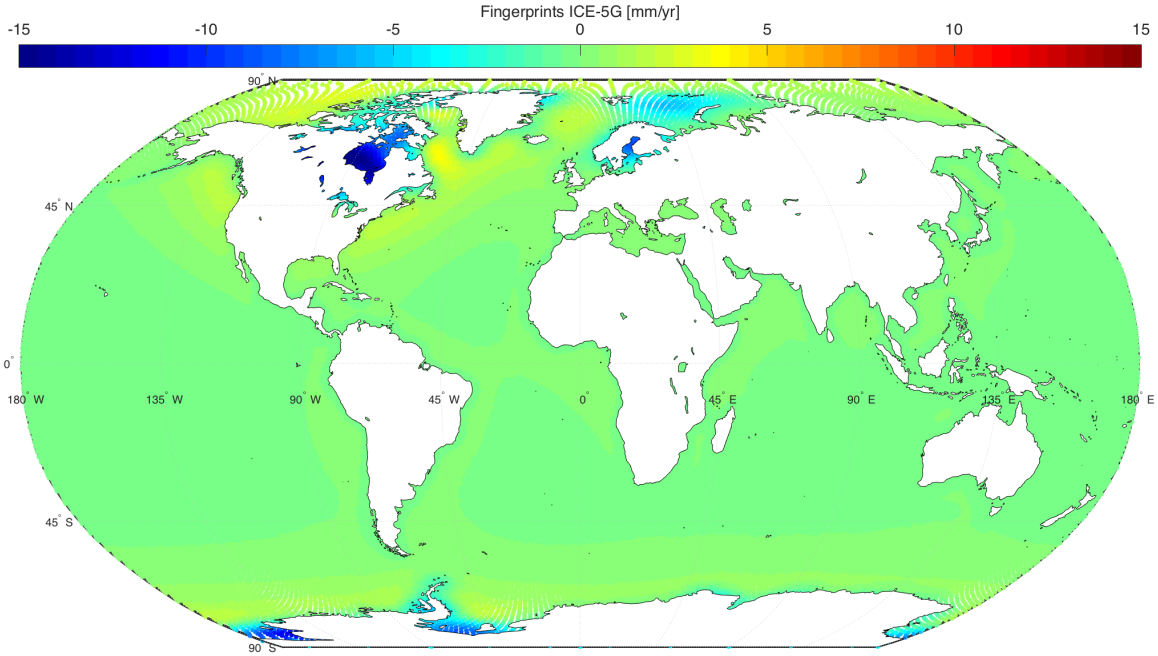

Figure 4.1.1: Present-day GIA-induced fingerprints from ICE-5G (21 kyr BP - present), as obtained by SELEN. The corresponding eustatic sea level change is in total 127.1 m (on average 5.8 mm/yr) (see also figure 4.1.4)

4.1.2 GIA-predictions from GRACE-observed ice melt

The elevation change by the ice-model constructed from the GRACE-observations from 2003-2014, ICE-GR, is shown in figure 3.2.3. As seen in figure 4.1.2, the ICE-GR model produces much smaller relative sea level change rates, than the ICE-5G model. In the area close to Greenland, which together with an small area in West Antarctica is experiencing the largest melt, the largest sea level change rates are seen ($\approx$ 0.1 mm/yr). Further away from the areas of ice-melt, there seems to be no or very small fingerprints.

4.1.3 Geoid changes and vertical uplift

The left panel in figure 4.1.3 shows the vertical uplift and change rate of the geoid for ICE-5G model. The geoid change ($\dot{N}$) is up to 15 times smaller than the vertical uplift in areas of large mass changes (Polar regions, Scandinavia and North America). The geoid rises when vertical uplift of land stores more

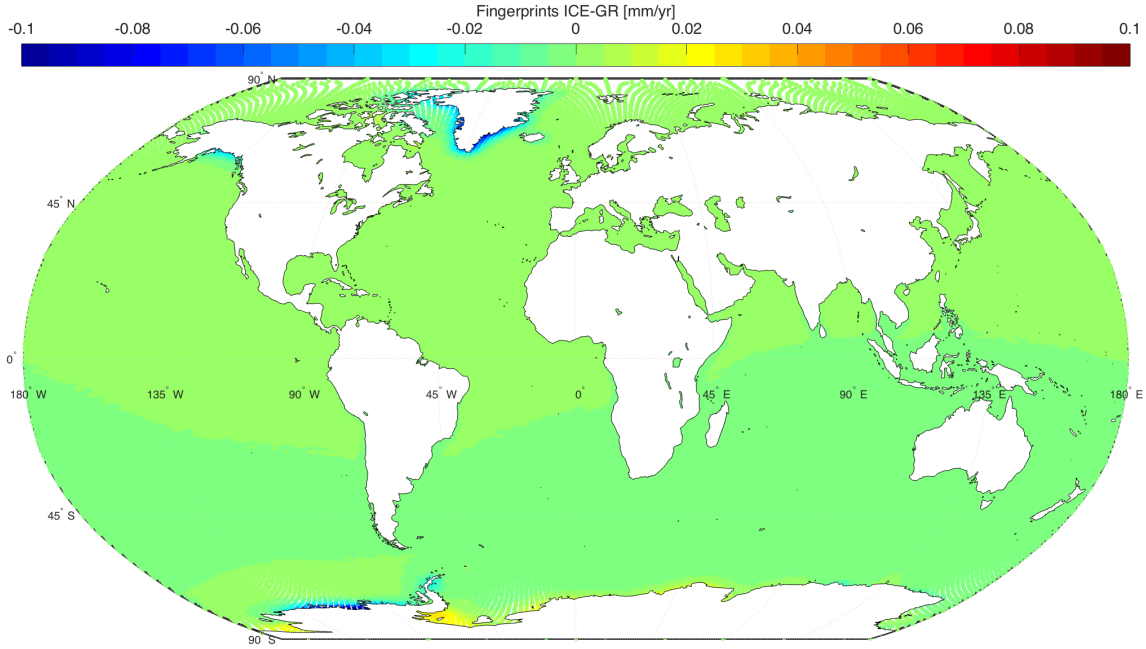

Figure 4.1.2: GIA-induced fingerprints from ICE-GR (2003-2014), as obtained by SELEN. The corresponding eustatic sea level change is in total 6.8 mm (on average 0.56 mm/yr) (see also figure 4.1.4)

mass above the reference ellipsoid and mantle material with large density is moved to the region (Farrel and Clark, 1976).

Further away from the mass loss (left panel of figure 4.1.3), does the geoid change has larger influence, accounting for almost half of the GIA-induced fingerprints ($2|\dot{N}| \approx \dot{S}$), which is in agreement with Stocchi et al, 2005[29].

A similar pattern is valid for the ICE-GR output (right panel of figure 4.1.3), even though the general change rates are 2-3 orders of magnitudes smaller, compared to the change rates from the ICE-5G model. This is in large contrast to Spada et al (2012)[28], that found vertical uplift rates of 2-4 mm/yr at the GrIS as an effect of the mass-loss measured by GRACE and up to 8 mm/yr when using ICESat data (Spada et al, 2012[28]).

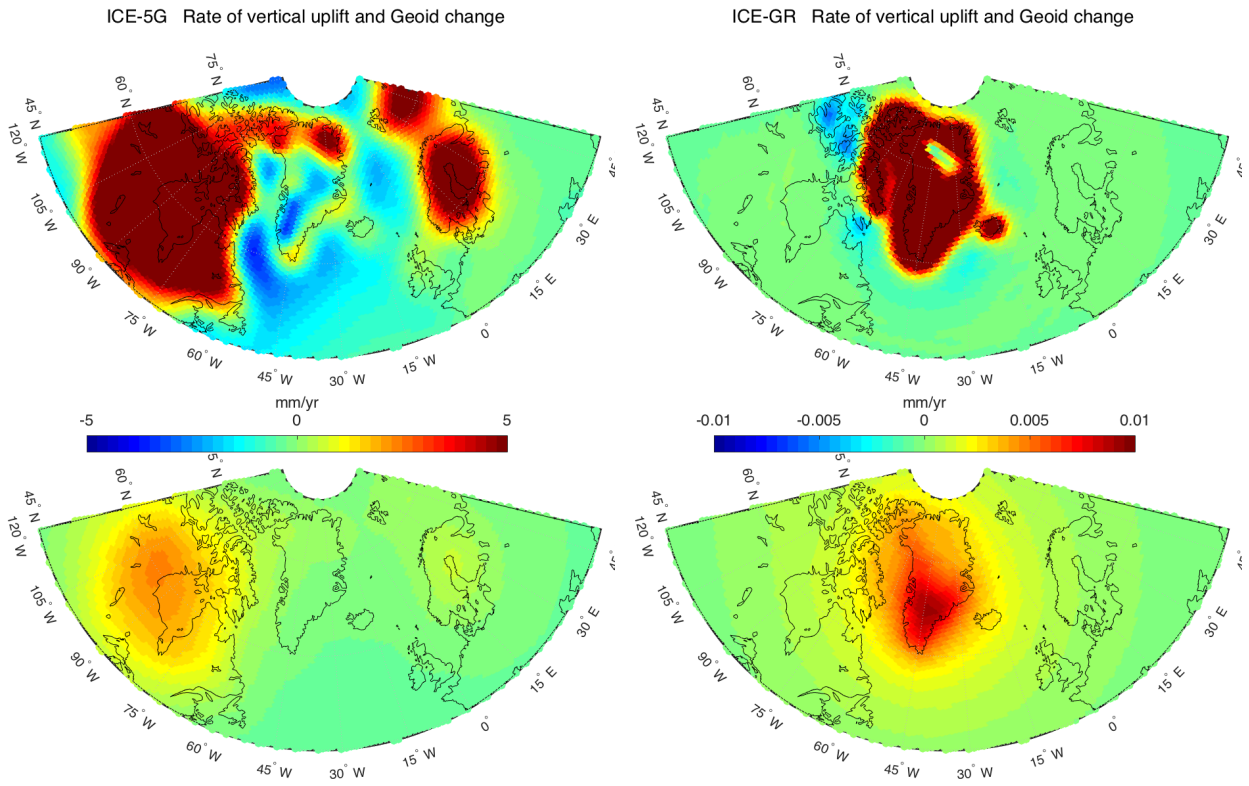

Figure 4.1.3: The present-day vertical uplift (top, $\dot{U}$) and geoid change rate (bottom, $\dot{N}$), for the ICE-5G model (left) and ICE-GR (right).

4.1.4 ESL-change from ICE-5G and ICE-GR

The eustatic sea level (ESL) change of the two global ice histories, ICE-5G and ICE-GR from SELEN is shown in figure 4.1.4. It shows that the ESL-change rate for the deglaciation since LGM 21 kyr is an order of magnitude larger than the present deglaciation. The ice-sheets of the ICE-5G-model melted completely 5-6 kyr ago, and today there is no land-ocean mass exchange from the ice-sheets at LGM (Waelbroeck et al. (2002)[33], Lambeck and Chappel (2001)[12]).

The average change rate of the ICE-GR provided by SELEN is 0.62 mm/yr (see figure 4.1.4), which is about half of the estimated global ice-melt contribution to present ESL-change found by other studies (Church et al, 2013[5], table 1.2.1).

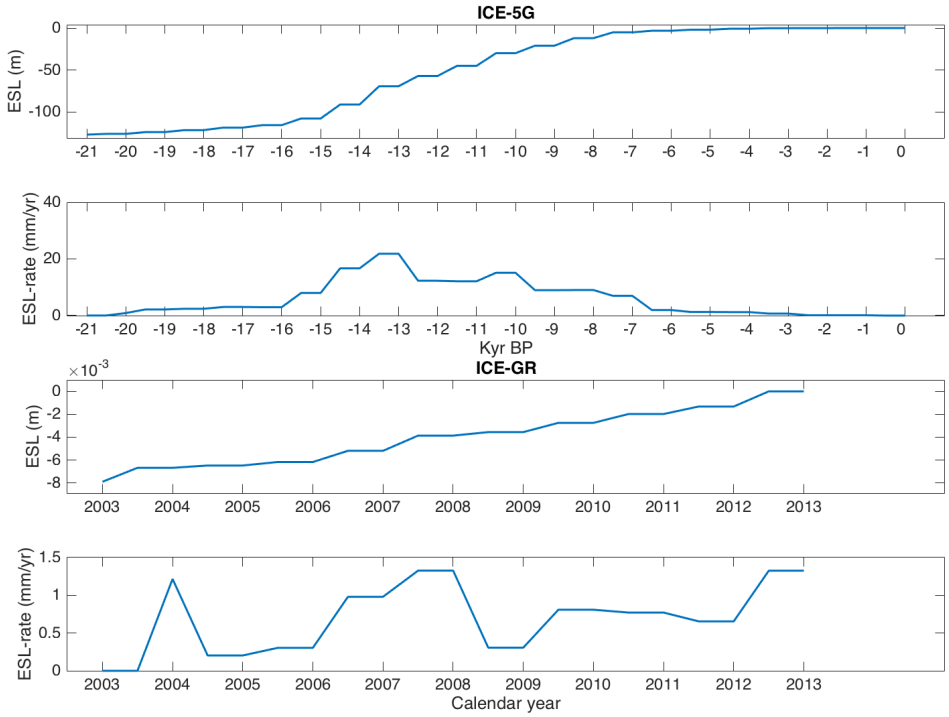

Figure 4.1.4: ESL-change and the change-rate for ICE-5G and ICE-GR as given by SELEN relative to present. The total ESL-change for ICE-5G is 127.1 m and for 6.8 mm ICE-GR.

4.2 GIA-predictions of GrIS-projections

In the same way SELEN is calculating the GIA-effect of the two pre-historic ice history models (ICE-5G and ICE-GR), GIA-predictions (fingerprints) of the four different projections of the GrIS (IMGRt, IMGRa, IM45, IM85) from 1990-2100 are used as input ice-models for SELEN. The Greenland ice-sheet (GrIS) is very vulnerable to climate change (a.o. Church et al 2013 5), thus in particular interesting to investigate for it's influence on future sea level rise. The 4 ice histories are described in section 3.3, and in figure 3.3.3 and 3.3.6. The temporal mass loss over the period for each projection is presented in figure 3.3.1 and the spatial mass loss for IMGRt and IMGRa can be seen in 3.3.3 and for IM45 and IM85 in figure 3.3.6.

4.2.1 Fingerprints from GrIS-projections

The most significant sea level changes will according to the GIA-theory occur in areas closest to the changing mass-load (Peltier, 2004, Spada 2011), which is also seen in the GIA-predictions of the ICE-5G (figure 4.1.1) and ICE-GR models (figure 4.1.2).

The figures (4.2.1, 4.2.2, 4.2.3, 4.2.4), presents the relative sea level changes around Greenland, together with the RSL-change of the whole world and the total elevation change of the GrIS for the four ice-histories between 1990 and 2100. The RSL-change around Scandinavia is used as an case example, in order to investigate the GIA-effect of the projected ice-melt of GrIS for the 21st century in a far-field.

The total mass change is comparable for the IMGRt, IMGRa and IM85 models ranging from 395 to 437 Gt/yr, but have very different spatial melt patterns.

The IM45 model has a total mass balance of 158 Gt/yr, which is somewhat below the present mass balance seen in the ICE-GR model (206 Gt/yr), but also differs spatially from the observed melt patterns by the GRACE-model.

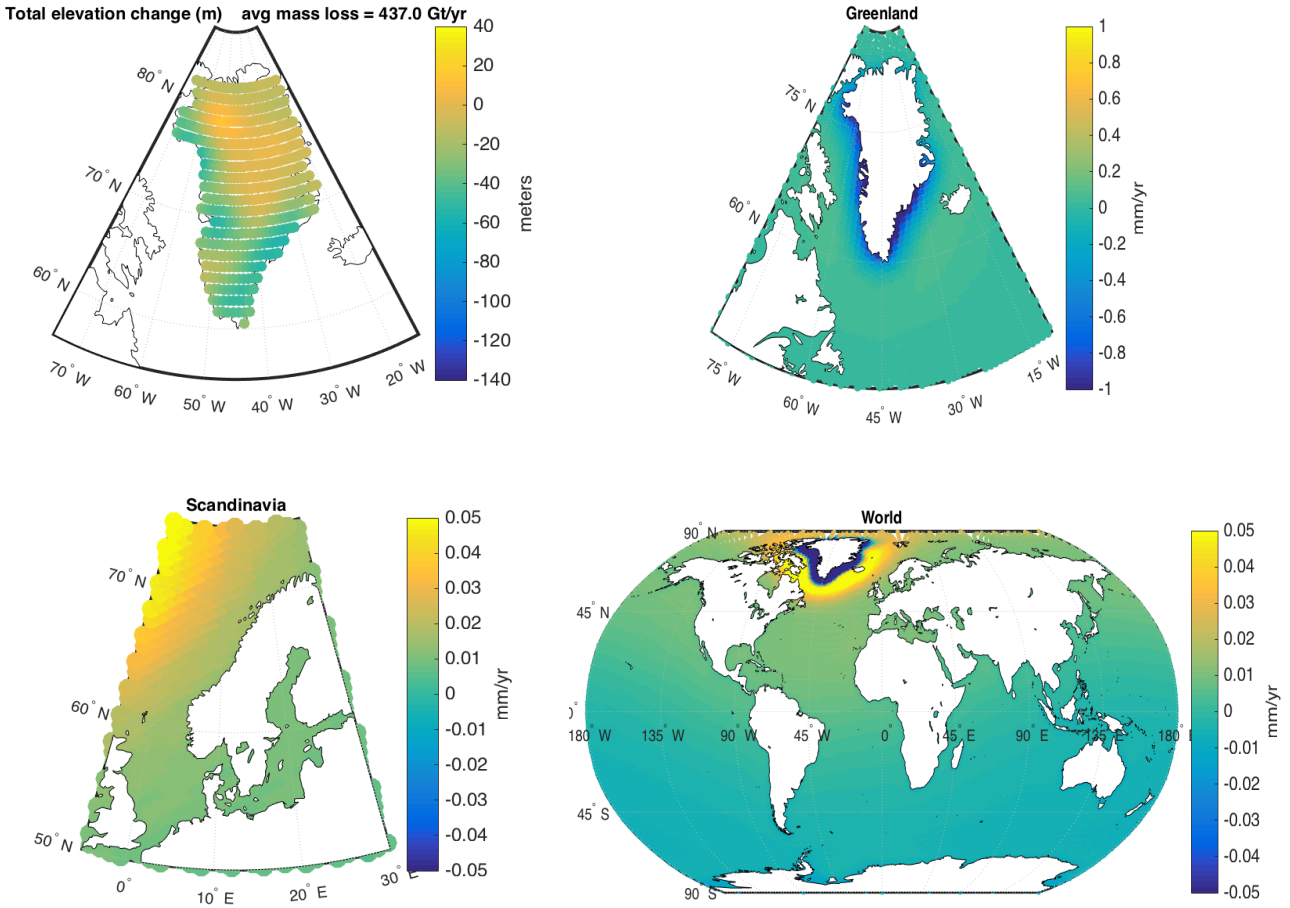

Figure 4.2.1: *Top left*: the total elevation change for GrIS for the ice history of **IMGRt** from 1990 to 2100. *Top right and bottom panel*: The relative sea level change (mm/yr, different scaled colorbars) in 2100 for IMGRt obtained by the GIA-predictions from SELEN around Greenland (top right), around Scandinavia (bottom left) and the whole world (bottom right). The corresponding total eustatic sea level change for the period is, according to the SELEN-output, 110.9 mm, or on average 1.01 mm/yr.

The largest fingerprints is at the source of ice melt, with rates up to -1 mm/yr (-0.5 mm/yr for the IM45-model). Just a few hundred kilometres away from the Greenland coastline does the GIA-effect almost vanish.

When using a smaller scale ($\pm$0.05 mm/yr), it is possible to see GIA-fingerprints around Scandinavia, showing an evident radial wave-pattern for all GrIS-projections, in particular visible for the IMGRa (4.2.2) and IM45

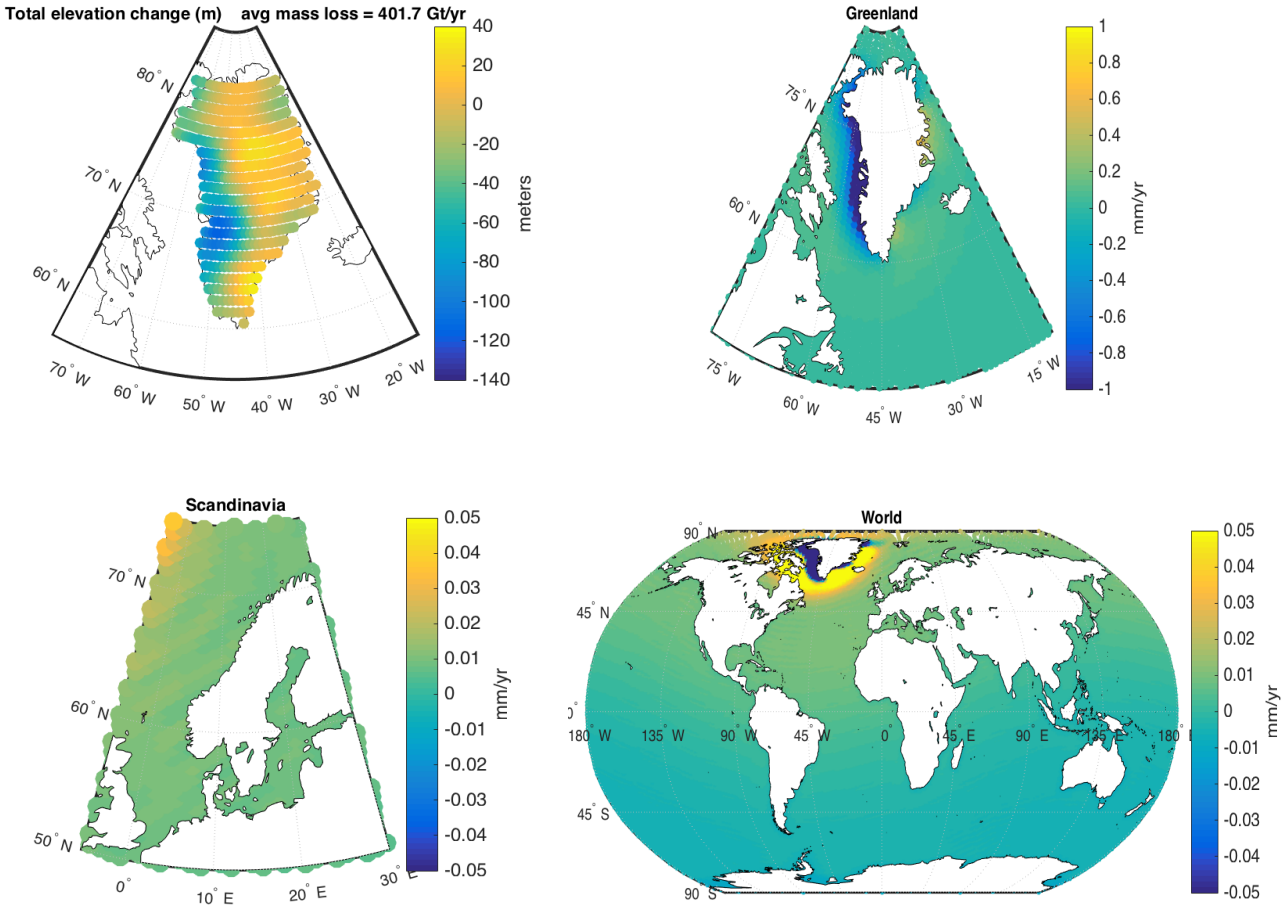

Figure 4.2.2: Same as in figure 4.2.1, but for the **IMGRa** ice model. The corresponding total eustatic sea level change for the period is, according to the SELEN-output, 102.6 mm, or on average 0.93 mm/yr.

model (4.2.3). Remarkable is that, the same two ice-models experience large differences between the east and west coast of Greenland, leading to the idea, that the wave-pattern is related to non-uniform melt of GrIS. The difference is less pronounced in the IMGRt and IM85-model (figure 4.2.1 and 4.2.4), which can explain an wave pattern that is more attenuated.

Figure 4.2.5 show horizontal cross-sections of the sea level rates along two latitudes for the four GrIS-projections. Again is a wave pattern for IMGRa and IM45 visible. It has a wavelength of about 500 km, an maxium amplitude of 0.005 mm/yr for IMGRa and 0.002 mm/yr for IM45. This is also

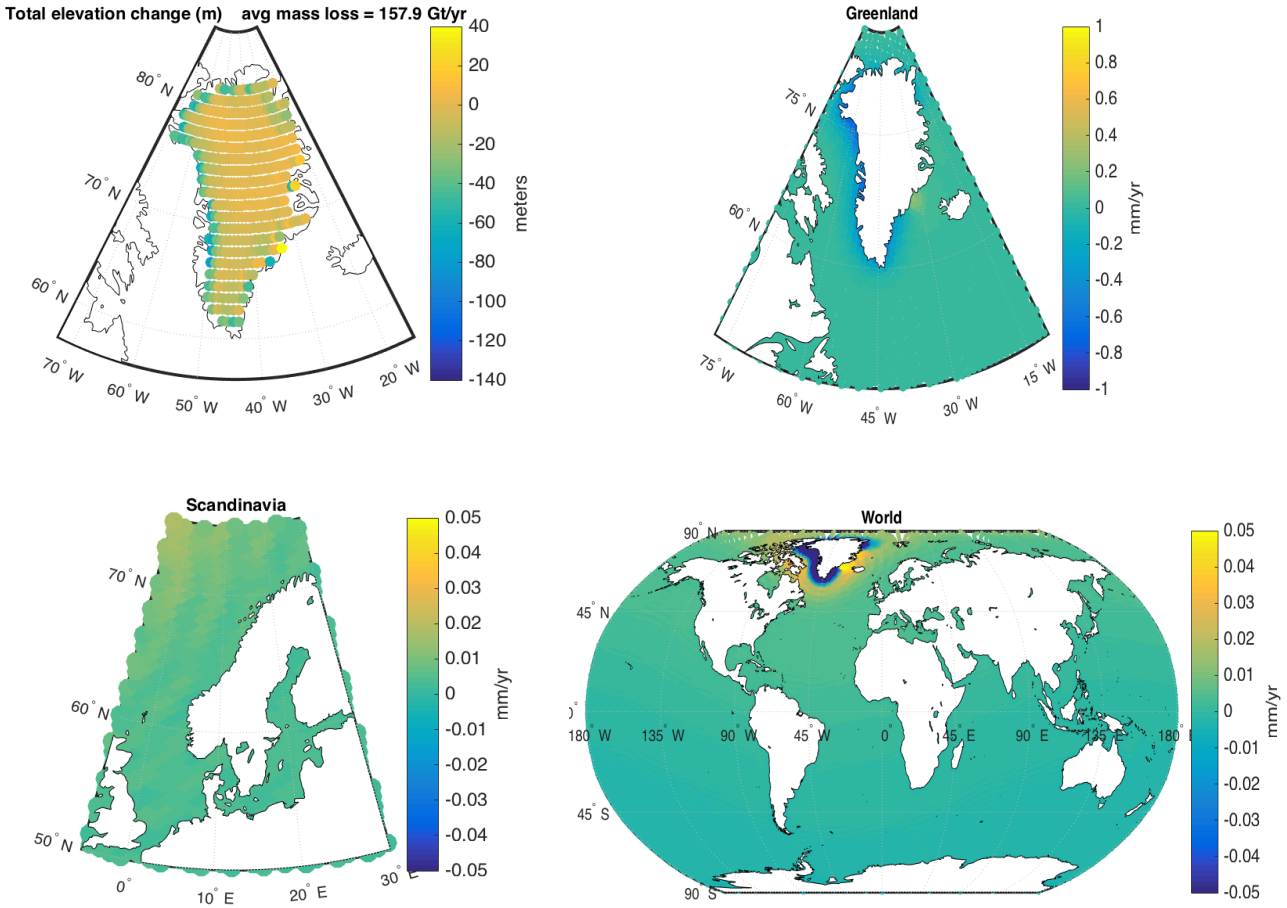

Figure 4.2.3: Same as in figure 4.2.1, but for the **IM45** ice model. The corresponding total eustatic sea level change for the period is, according to the SELEN-output, 41.6 mm, or on average 0.38 mm/yr.

seen in the regional maps in figure 4.2.3 and 4.2.2.

Also visible in figure 4.2.5 and in the global maps of figure 4.2.1 - 4.2.4, is a bulge of positive relative sea level rates, topping around 500 km off the Greenland coast with rates of up to 0.1 mm/yr (for IMGRt, IMGRa and IM85). This is well in line with the GIA-theory (Mitrovicia, 1991 a.o. [16]), where mantle material surrounding the source of ice melt is moved towards the centre of the ice-melt causing a subsidence in the surrounding peripheral oceans, and subsequently (due to the SLE (Farrell and Clark 1976[7])) resulting in a relative sea level rise.

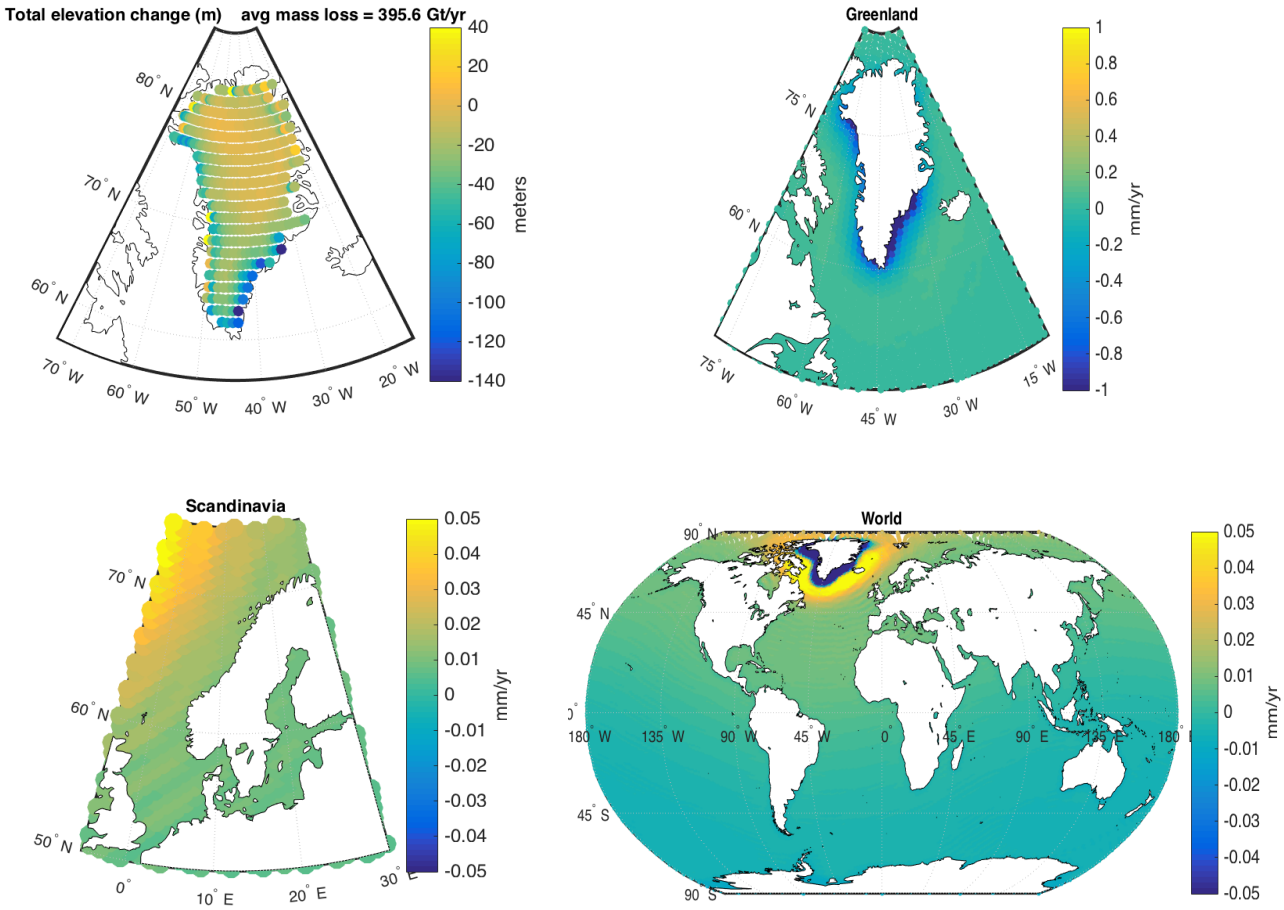

Figure 4.2.4: Same as in figure 4.2.1, but for the **IM85** ice model. The corresponding total eustatic sea level change for the period is, according to the SELEN-output, 98 mm, or on average 0.89 mm/yr.

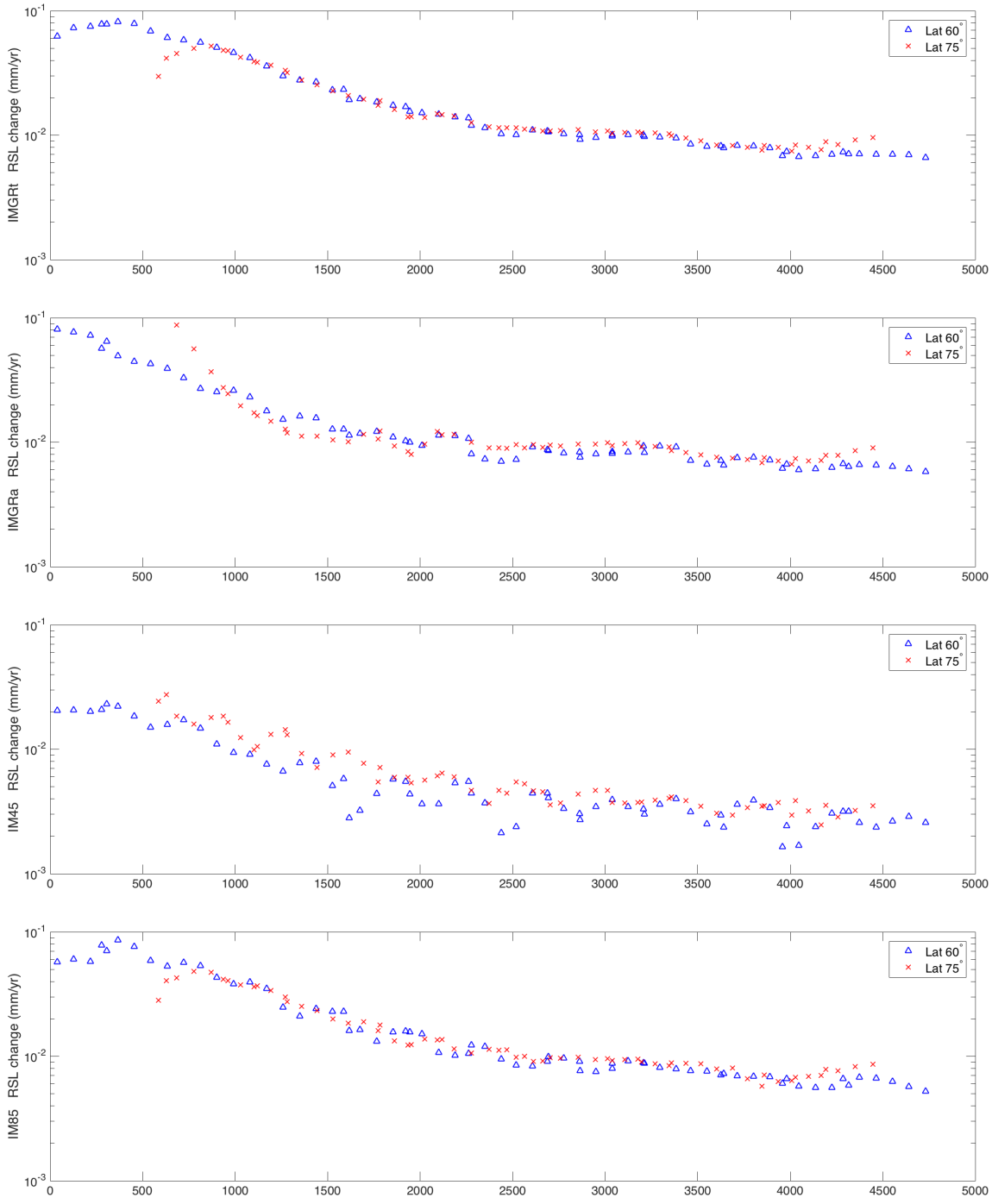

Figure 4.2.5: Cross-sections of the relative sea level change rate in mm/yr for the 4 GrIS-projections along latitude 60° (blue triangles) and 75° (red crosses). The x-axis denotes the distance in km from longitude -35° W at the Greenland west coast. The RSL-change rate is on a logarithmic scale ranging from 0.1 mm/yr to 0.001 mm/yr.

4.3 GrIS-GIA contribution to sea level change at Denmark's coastlines

As seen in figure 4.1.2, the present day ice melt, causes a very small GIA-effect in a far field, compared to the ongoing GIA-effect from the LGM (figure 4.1.1).

As an example, we will look at the GIA-effect at the Danish coastline (approximately 2500 km off the Greenland east-coast). The GRACE-model of last decades mass change is shown in the right panel of figure 4.3.1, and reveals that the GIA-induced RSL-change is between $5-7\times10^{-4}$ mm/yr, and significant smaller than GIA-effect from the LGM (the ICE-5G ice history), which still today is affecting the region around Denmark between -2 and 0 mm/yr (left panel of figure 4.3.1).

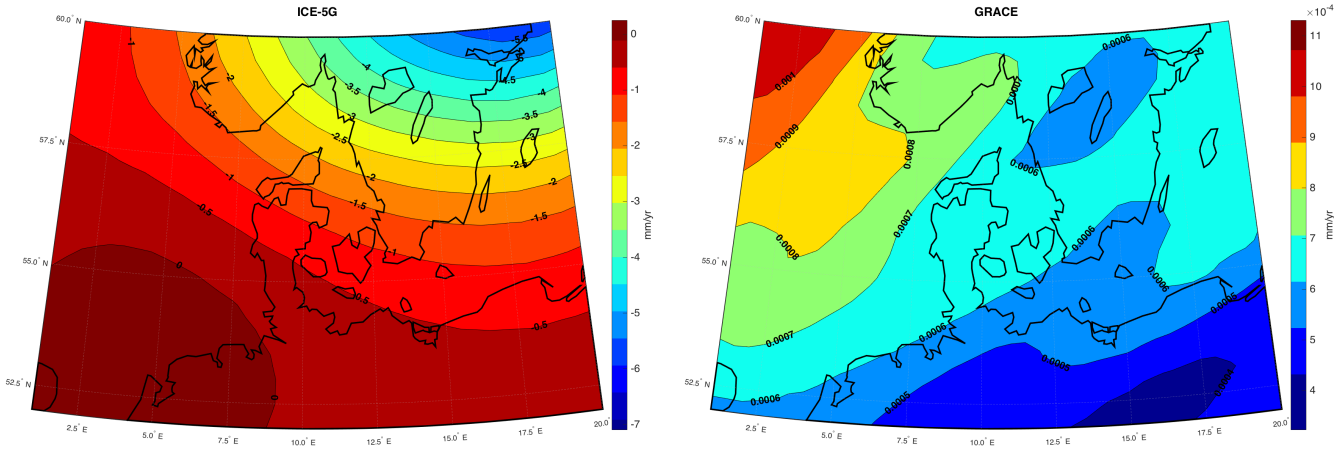

Figure 4.3.1: Present-day GIA-induced RSL-change rate in mm/yr for ICE-5G (left) and ICE-GR (GRACE) (right).

The RSL-rate for GrIS-projections is ~ 0.01 mm/yr (shown in figure 4.3.2), which should be compared to the corresponding ESL-rate, that is in the order of 1 mm/yr and thus 2 orders of magnitude larger.

If we neglect the uncertainties and the small scale of the effect, the general picture is that the deglaciation of the GrIS contributes *positively* to a sea level rise. The IMGRt, IMGRa and IM85 models with comparable mass

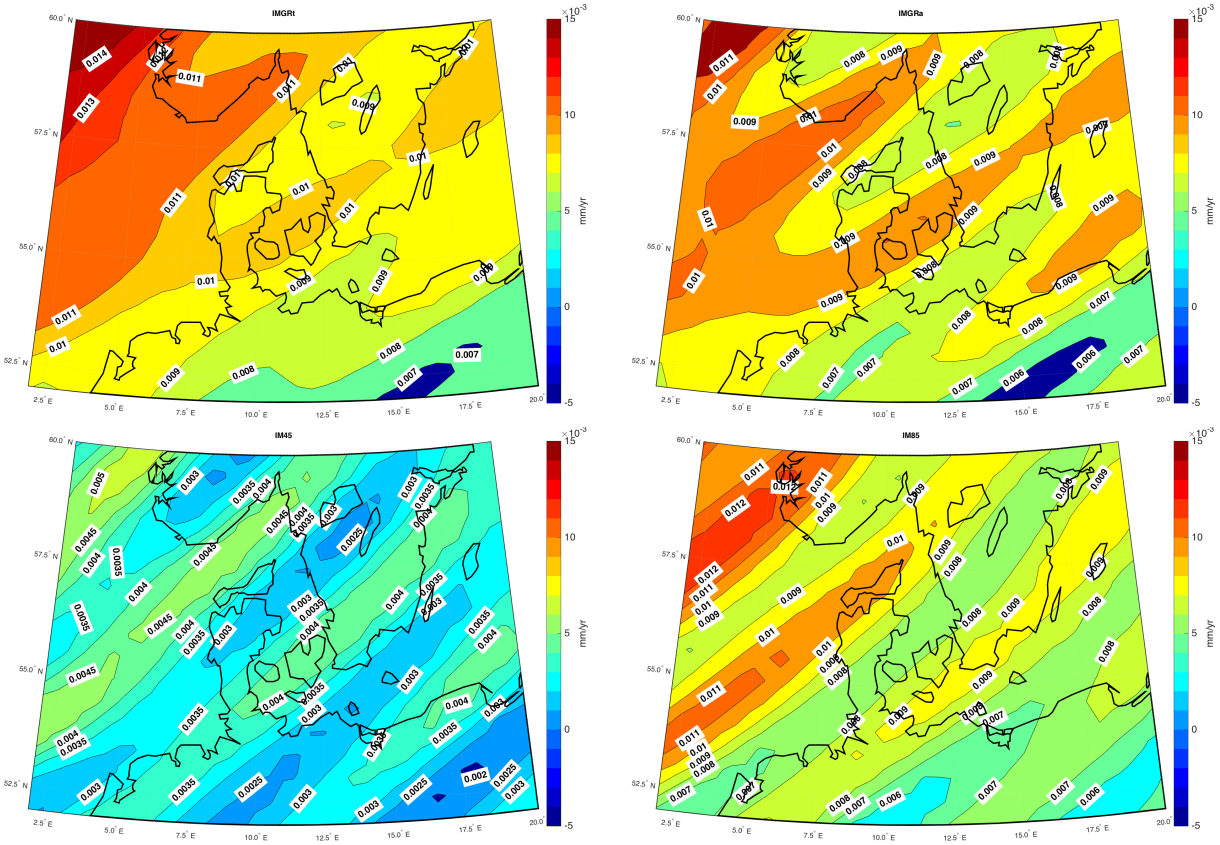

Figure 4.3.2: RSL change rate in 2100 (mm/yr) for the 4 GrIS-projections. From top left: IMGRt, IMGRa, IM45 and IM85

losses of the GrIS, show similar patterns of GIA-effect. It may be estimated, that a mass loss of between 390-440 Gt/yr of the GrIS over a time-period of 110 years, gives a GIA-effect along Denmarks coastlines between $8-11\times10^{-3}$ mm/yr. For the IM45-model, with an average mass loss of around 170 Gt/yr, the GIA-effect is between $3-4\times10^{-3}$ mm/yr, which is five times larger than the present-day change rates in the same region from ICE-GR (right panel figure 4.3.1).

Also in figure 4.3.2 the wave pattern is detected, which also was seen before and will be discussed further in the discussion-chapter.

Chapter 5

Discussion

The estimated GIA-effect on the relative sea level from the different ice histories depends on a number of assumptions and simplifications.

First, the ice-histories in ICE-5G are model estimations (Peltier, 2004 [22]), and the GrIS-projections are mostly based on statistical projections instead of physical assumptions. In particular, any predictions of the dynamic ice loss of the GrIS is connected to large uncertainties (van der Broecke et al., 2009[2]).

Secondly, the VM2 earth-model parameters is a simplified uniform five layer model, whereas in fact there are large local variations, with different impact of the GIA-theory (Mitrovica et al. 2005[18], Nakada et al, 2015[19]).

Thirdly, other short and long-lived regional sea level effects, not accounted for in the GIA-theory, can possibly be overshadowing the results seen from GIA (Bamber and Riva, 2010[1]).

5.1 Uncertainties connected to GrIS mass balance

The results in figure 4.3.2 are varying accordingly to the different mass-balance histories used. A study by Fuerst et al (2015)[9], estimates the ice discharge in 2100 to be between 400 and 1100 Gt/yr, depending on the ocean temperature increase (figure 5.1.1), which is more than the dynamic ice loss projected in the ice models (see figure 3.3.1). Same paper states the present dynamic ice-loss to be between 356 and 371 Gt/yr, which corresponds to the dynamic ice loss used in this study, when the modelled SMB-predictions are subtracted from GRACE-data.

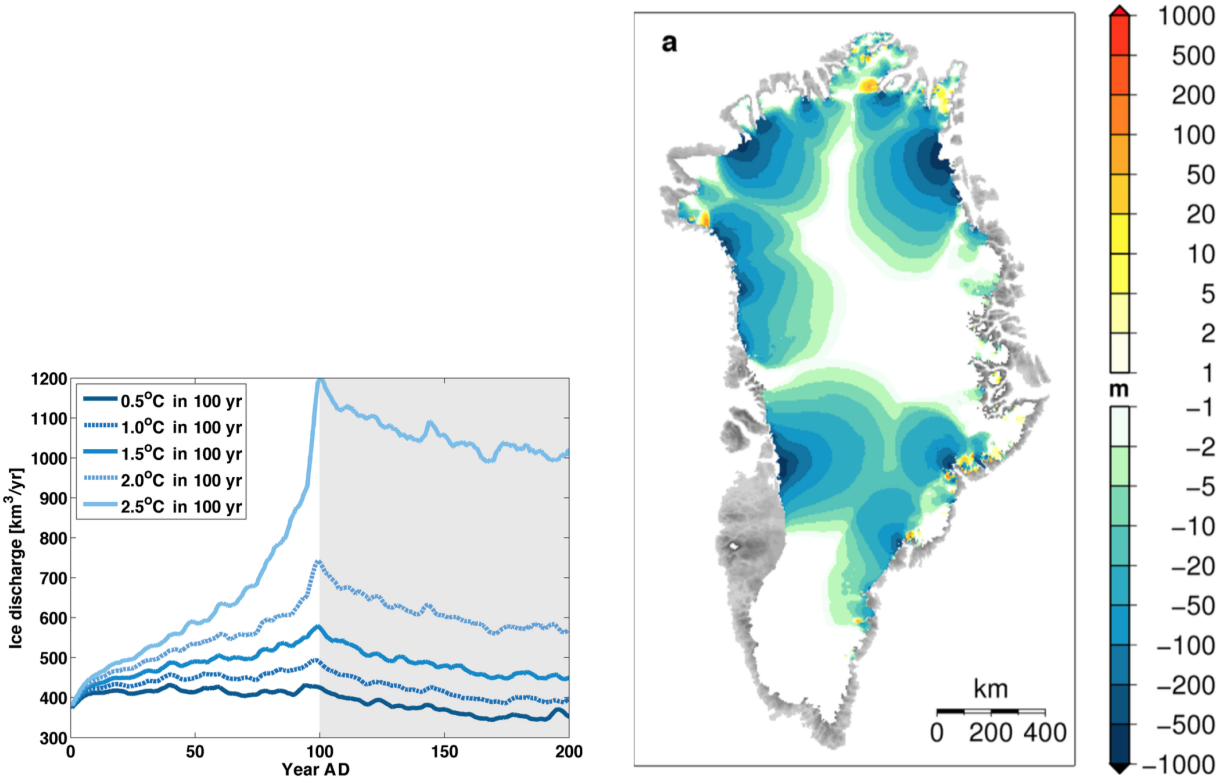

Figure 5.1.1: Left: Ice discharge response to a linear increase in ocean temperature by Fuerst et al (2015)[9]. Right: Ice discharge in 2100 corresponding to a medium warming scenario by Fuerst et al (2015)[9].

The GrIS-projections correspond to an ESL-change rate, which are presented

in table 3.2.1. The ESL-rate is 0.38 mm/yr for IM45 and 0.89, 0.93 and 1.01 mm/yr for the IM85, IMGRa and IMGRt, respectively. An ensemble analysis by Yan et al, 2014[35] of the CMIP5 (Climate Intercomparison Project 5)-models reveals a future contribution of GrIS between 0.2 and 0.8 mm/yr for the RCP 4.5 scenario and 0.5 and 1.1 mm/yr for the RCP 8.5 scenario, which indicates that the GrIS-projections used in this study, at least in terms of total mass loss, is within the physical predictions. The same study predicts, if the basal sliding driving the ice discharge is double the current level, the mentioned sea level rates will double, underlining the uncertainty and importance of the dynamic ice loss.

5.2 Uncertainty of GIA-predictions

5.2.1 Earth parameters

The earth model parameters from the VM2 rheological profile used in this study are shown in table 3.1.1. This is a simple 5-layer model, and since the release of the current version of SELEN, a new ice history, the ICE-6G ice model (Peltier, 2015[23]), that uses an improved VM5a viscoelastic profile has been published.

When subtracting the ICE-6G with the ICE-5G RSL-rates (figure 5.2.1), it reveals a difference of up to 5 mm/yr in some areas, which corresponds to an variation of about 30 %. This can be compared to Argus and Peltier (2010), that found rates of the vertical uplift differ with 1-3 mm/yr, when comparing the VM5a with the VM2-model. An recently published paper by Purcell et al (2016), applies the ICE-6G model to the Australian National University (ANU) CALSEA software (Lambeck et al. 2003), with resulting RSL-rates with a discrepancy of between 2 and 8 mm/yr when compared to RSL-rates published by Peltier (2015).

Spada et al. (2012)[28] (figure 5.2.2) used the SELEN program to analyse the GIA-effect around Greenland for the ICE-5G model with 4 different viscoelastic profiles, and found local variations of up to 5 mm/yr.

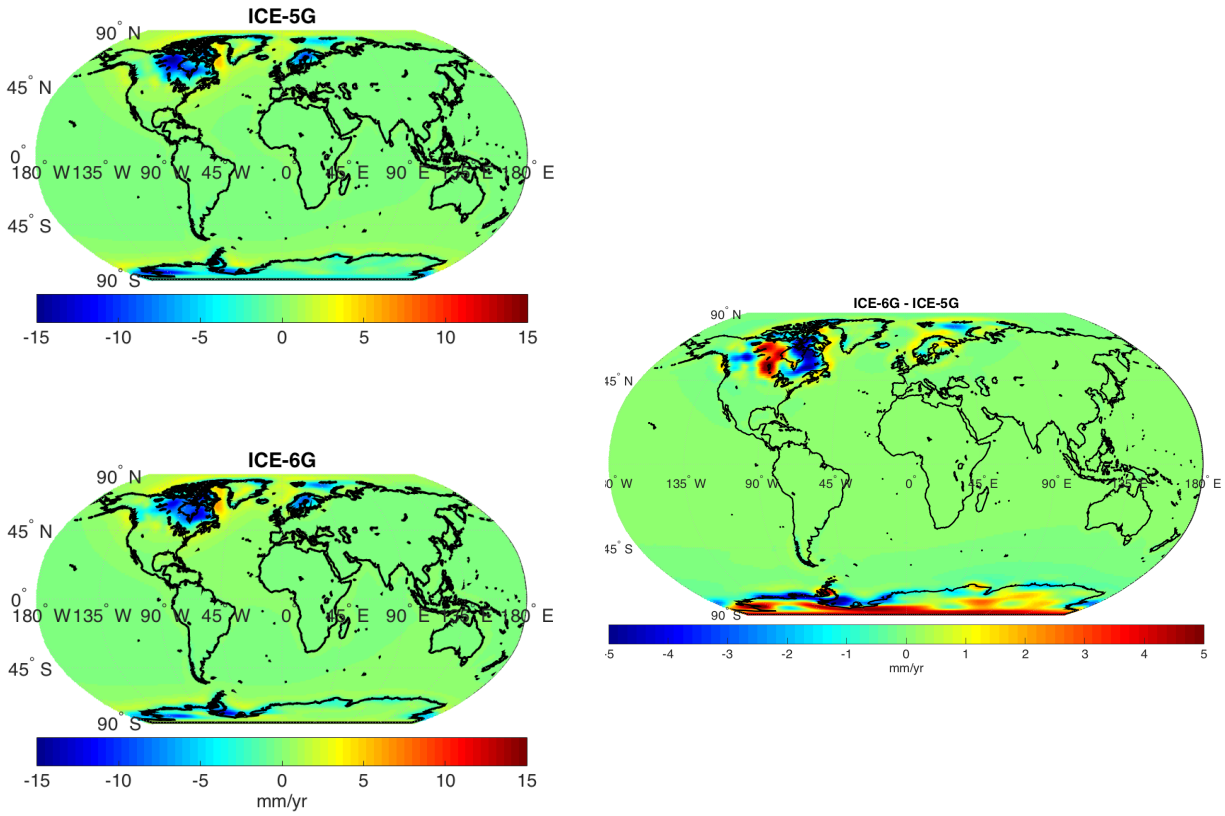

Figure 5.2.1: Present sea level change rates for ICE-5G(VM2) and ICE-6G(VM5a). The difference of the two ice-models is shown on the right.

5.2.2 Long term GIA-predictions

As seen in figure 5.2.2 and other studies, different earth models can locally have large GIA-variations. When comparing the total RSL-change from SELEN since the LGM (ICE-5G-model) with in-situ observations, there is a discrepancy of several meters (up to 15 %, Spada and Stocchi, 2012[28], figure 5.2.3).

Fennoscandinavian uplift

Model-variations found by Cathles (1975)[4] compared to observations (figure 5.2.4), suggest a variation of the Fennoscandinanvian uplift of 1 mm/yr. An estimate for the ICE-5G GIA-effect around Denmark (shown in figure

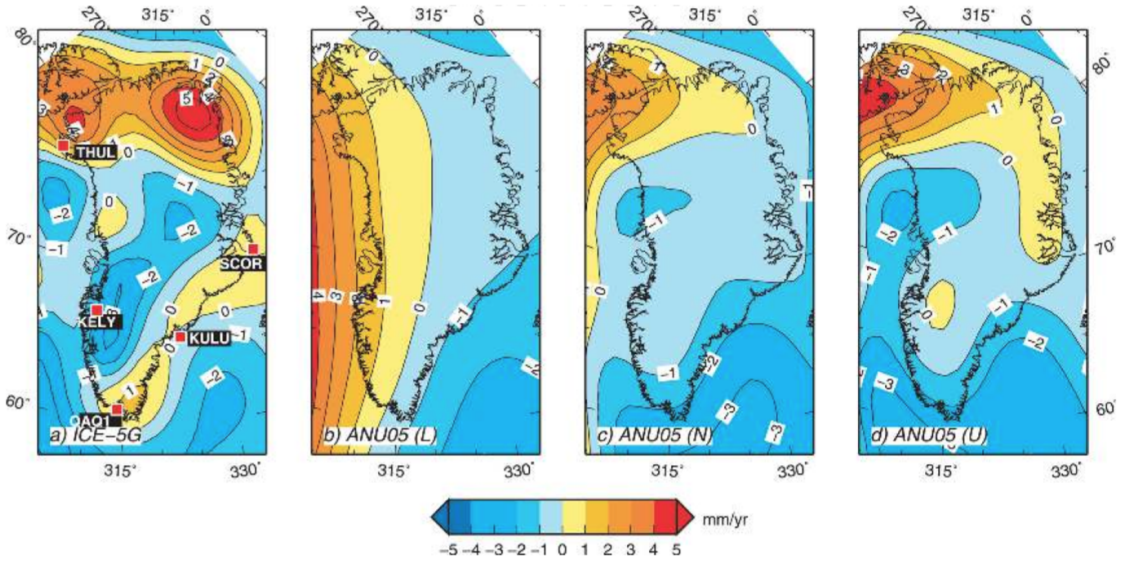

Figure 5.2.2: Present-day GIA uplift rates computed with ICE-5G ice model with four different rheological models. Panel (a) is similar to this study. From Spada et al., 2012

4.3.1) is therefore more likely -1 to 1 mm/yr in the south west, and 1 to 3 mm/yr north-east of Denmark, in conformity with other studies of the present GIA effect of the Fennoscandinavian deglaciation (Timmen et al., 2011[32], Ågren and Svensson, 2007[36]).

SELEN reliability

In general, does the SELEN-output align with other GIA-RSL-analysis (e.g. Peltier, 2004[22], Mauz et al 2015[14]) of the ICE-5G ice model, and is sufficient to say, that SELEN-configuration used in this study is able to predict trust-worthy GIA-predictions from the sea level equation (SLE, Farrel and Clark 1976[7], Mitrovicia 1991[16], Spada and Stocchi 2006[26]).

5.2.3 Short-term predictions

The short-term GIA-predictions from ICE-GR and IMGRa, IMGRt, IM45 and IM85. The changes are often covering smaller area (as compared to the

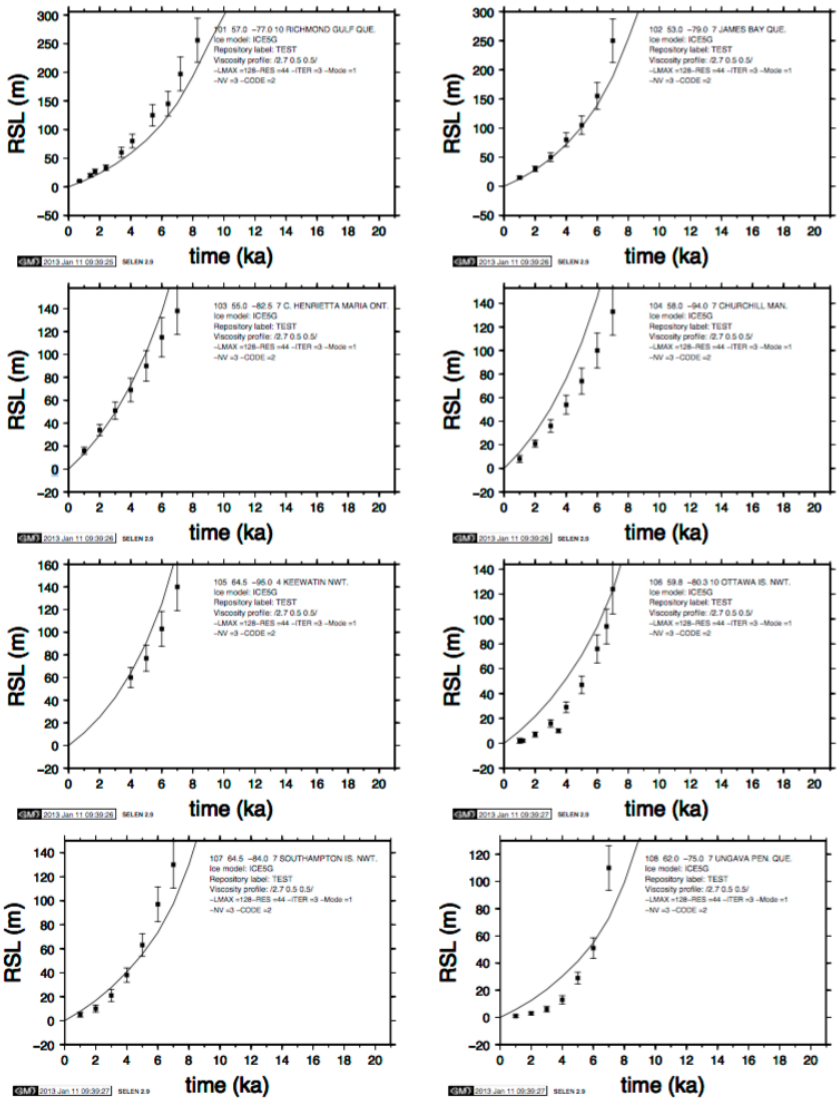

Figure 5.2.3: RSL outputs from SELEN compared to observations, from Spada and Stocchi (2012)[28]

ice sheets during LGM), and thus the load changes mainly affect the upper lithosphere, and thus less dependent on the rheology of deeper layers and the general rheological profile (table 3.1.1).

The elastic effect for the GrIS is measured with GPS-stations around Greenland (Khan et al., 2007[10], Nielsen et al. 2014[20]), have rates of 2-9 mm/yr

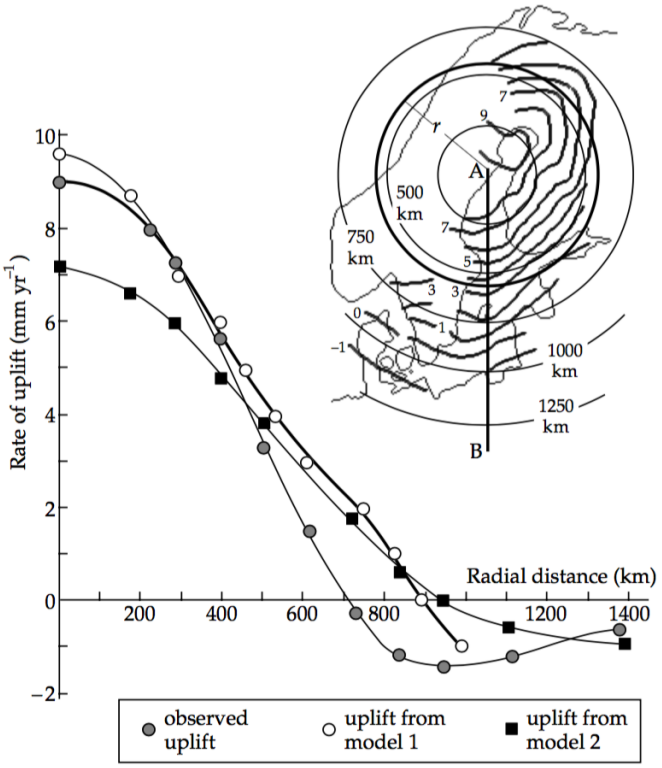

Figure 5.2.4: Comparison of Fennoscandian uplift rates interpreted along profile AB with uplift rates calculated for two different models of mantle viscosity (from Cathles (1975)).

and is often larger than the current GIA-effect from the LGM in this area and the global ESL-change (Spada et al 2012[28]). The GIA-effect on Greenland of the current melt, as found in this study by SLE is at maximum 0.1 mm/yr.

The SLE solves the viscoelastic GIA-effect that is connected to deglaciation (Spada and Stocchi, 2006[26]). In Spada et al 2012[28], where only the vertical displacement of elastic deformation is used to analyse the relative sea level from present-day GrIS-melt (191 $\pm$ 23 Gt/yr), results in sea level changes between -4 and -8 mm/yr along the Greenland east coast and rates of up to 0.5 mm/yr in the far field (around Denmark), which is 3 magnitudes larger than the GIA-results of ICE-GR (figure 4.1.2).

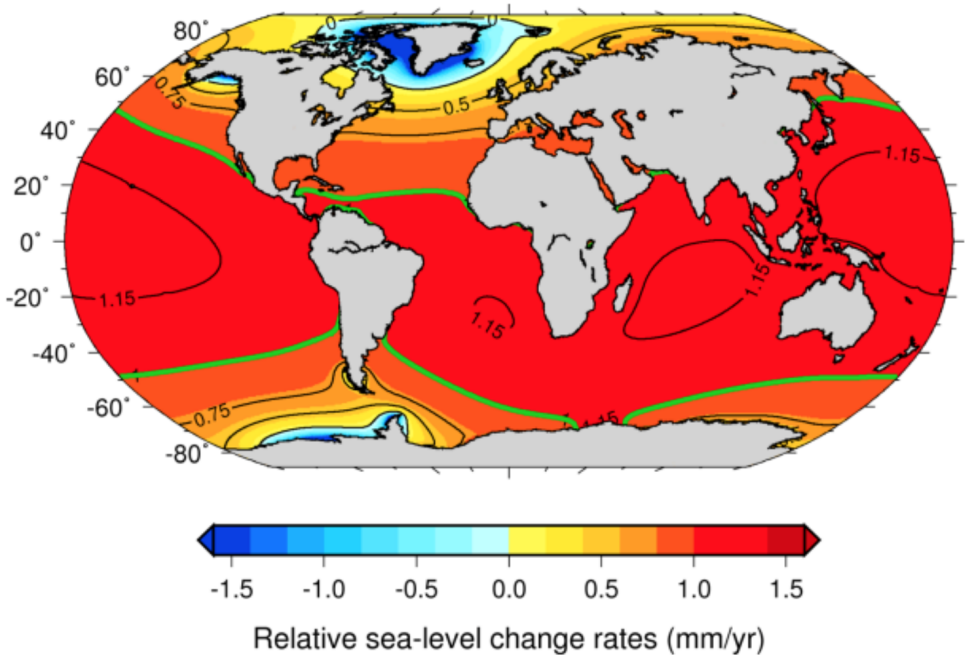

Figure 5.2.5: Relative sea-level change rates from present change of ice masses. The green line indicates the ice sheet's contribution to eustatic sea level change rate (1.4 mm/yr). From Bamber and Riva (2010)

This indicates, that the viscoelastic effect, and the corresponding Greens Functions does not have significant influence on short time scales, when comparing to the immediate elastic response (which is *not* a part of the SLE).

The RSL-changes in the far field seen by Spada et al. (2012)[28] (figure 5.2.6) and Bamber and Riva (2010)[1] (figure 5.2.5) are caused by gravitational adjustments connected to the vertical uplift and the different mass distribution when ice is transformed into ocean water (Woodward, 1888[34], Bamber and Riva, 2010[1]).

Only very few sea level studies are considering the GIA-effect of recent and future ice melt, and there is to the knowledge of this author no studies showing the GIA-effect of recent GrIS melt or of future deglaciation scenarios of the GrIS, making it difficult to validate the results for the short term GIA-

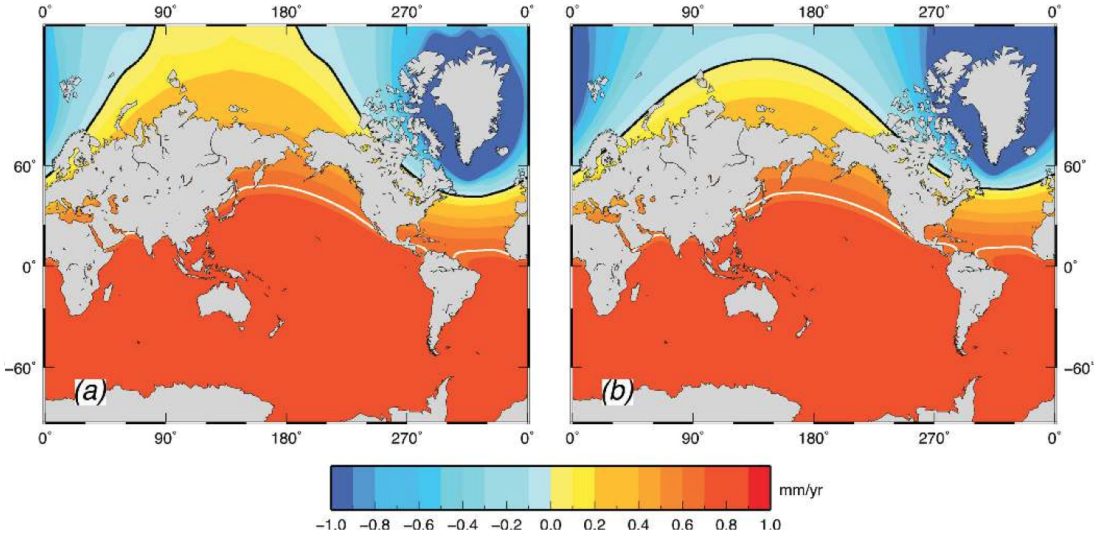

Figure 5.2.6: Rate of global sea level variation associated with the M3 GrIS ice model (a) (from Sørensen et al, 2011[31]). b) has the same total mass loss as M3, but with uniformly spatial melt. The white line indicates the eustatic sea level ($\approx 0.67mm/yr$). From Spada et al., 2012[28]

predictions.

The general picture is that the GIA-effect, is a 1-3 orders of magnitudes smaller than the current relative sea level rates connected to ice melt. Bamber and Riva (2010)[1] are describing the GIA-effect from recent ice melt as insignificant, and therefore not taking it into account, when predicting the RSL-rates (figure 5.2.5).

The GIA-effect of the GrIS-projections that spans 110 years is at most effecting the coastline around Greenland with a sea level rate of -1 mm/yr, which is 15-20 % of the current sea level rates seem in the same area by Khan et al, 2007[10] and Spada et al., 2012[28], making the estimates significant enough to be considered when discussing sea level in the area around Greenland. The GIA-effect is highly dependent on the ice model (M. Perrette et al, 2013[24]) and since the ice-projections for the GrIS used in this study is non-physical, no detailed analysis is made of the GIA-effect around Greenland.

The sea level further away from the source of mass loss, is less dependent on the spatial mass loss distribution of the GrIS (Spada et al. 2012[28], Bamber and Riva 2010[1]). This is also seen in the figure 4.3.2 of the coastal region around Denmark, where the RSL-rates of 3 GrIS-projections (IMGRt, IMGRa, IM85) with comparable mass loss are showing the same rates between 8-11$\times 10^{-3}$ mm/yr. It is though, noteworthy, that the IM45 ice model, which is representing an "mild" climate scenario is showing RSL-rates between 3-4$\times 10^{-3}$ mm/yr. This indicates, that the total mass loss is the dominant driver for the GIA-effect, rather than spatial mass balance differences on the ice-sheet.

The RSL-wave pattern seen in figures 4.3.2, 4.2.2, 4.2.5, is in the range of 10-20 % of the total RSL-effect. It is not found in other studies of the viscoelastic effect, and is probably a result of the non-uniform melt of the GrIS-projections. When comparing the vertical uplift and the change of the geoid for the IMGRa-model in figure 5.2.7, it is clear, that it is the vertical deformation of the lithosphere that is causing this pattern. The geoid decreases radially, whereas the vertical uplift has a non-uniform pattern, and when subtracted from the geoid, results in the sea level change wave-pattern shown in figure 4.3.2.

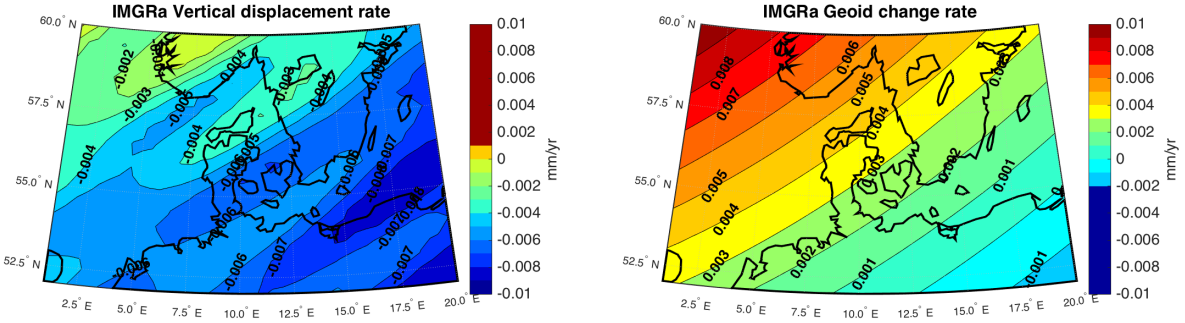

Figure 5.2.7: Change rate of the vertical displacement (left) and the geoid (right) for the IMGRa-model.

Considering the study from Bamber and Riva (2010)[1], it is reasonable to order the total mass loss of GrIS as the largest driver of the GIA-effect, and the influence of a non-uniform ice-distribution on the GIA-effect is only

secondary and barely relevant when discussing RSL-effect from future GrIS-melt. It does, though, contribute to the overall uncertainty.

Chapter 6

Conclusions and suggestions for further studies

The sea level equation (Farrell and Clark, 1976) provides 'fingerprints' of the glacial isostatic adjustment (GIA), given a certain ice chronology and a rheological profile. By using the SEa Level EquatioN solver, SELEN 2.9 (Spada and Stocchi, 200626), SLE has been numerically solved for four different Greenland ice sheet (GrIS) projections to assess the effect of the glacial isostatic adjustment (GIA) on future sea level rise.

In order to validate the method, the SELEN-configuration is used on the ICE-5G ice history from last glacial maximum (LGM) to present, developed by Peltier (2004). The calculated present-day relative sea level (RSL) rates are in line with other RSL-studies using the ICE-5G model (Peltier 2004, Toscano 2011), and confirms the strong viscoelastic uplift of 10-15 mm/yr seen in parts of the Northern Hemisphere, causing a sea level fall.

The SLE only solves the viscoelastic post-glacial rebound of the mantle and crust, whereas the immediate elastic rebound of the lithosphere following an change in surface load, is not considered in SLE (Farrell and Clark 1976, Mitrovicia 1991, Spada 2012). This enables SLE to give GIA-predictions of the delayed viscoelastic rebound for glaciation chronologies of much smaller

time-scale, i.e. present ice mass loss detected by for example the GRACE satellites. A case using the GRACE ice chronology, the ICE-GR model, as input to SELEN is therefore also conducted to assess the GIA effect on a relatively short time-scale (12 years).

The SELEN output of ICE-GR confirms other studies (Bamber and Riva, 2010 a.o.), that the GIA-effect of present ice loss is negligible. Except close to the mass loss, the rates are in the magnitude of 5×10^{-4} mm/yr, which is 3 orders of magnitudes smaller than the corresponding ESL-change (0.62 mm/yr).

The GIA-induced RSL-rates of the four projections of the Greenland ice sheet (GrIS) from 1990-2100, IMGRt (ESL: 1.01 mm/yr), IMGRa (ESL: 0.93 mm/yr), IM45 (ESL: 0.38 mm/yr) and IM85 (ESL: 0.89 mm/yr) are at least one order of magnitude larger. Around Greenland the viscoelastic effect of the ice melt is $\simeq -1mm/yr$ (-0.5 mm/yr for IM45) in 2100, contributing to the RSL-fall of the elastic rebound (Khan 2007, Spada 2012) occurring during the mass loss.

The GIA-predictions for a 'far field' region, the case example of Denmark, are between 8-11$\times10^{-3}$ mm/yr for IMGRa, IMGRt and IM85 and 3-4$\times10^{-3}$ mm/yr for IM45. In magnitude, this is much less than the current RSL-contributions from the GrIS in the same region (between -0.1 and -0.3 mm/yr), estimated by Bamber and Riva, 2010, and Spada et al. 2012 and the GIA-fingerprint from LGM (between 0 and -2 mm/yr).

A wavepattern with amplitude 10-20 % of the RSL-change and a wavelength of about 500 km is detected for in particular the IM45 and IMGRa, radially propagating from GrIS. This is possible due to the the spatial non-uniform melt of the GrIS-projections, but has to be confirmed with further studies.

The much larger viscoelastic rebound after 110 years in the GrIS-projections is, when compared to the 12 years of GRACE-observations from ICE-GR, indicating an increasing influence of the delayed viscoelastic rebound after ice melt of GrIS with time. The size of the remaining rebound, and hence

the true 'fingerprints' of the GIA-effect, can further be investigated by developing scenarios with longer time span ($\sim$ 1 kyr), where the GrIS obtains mass balance.

Acknowledgements

The author wants to thank Peter L. Langen from the Danish Meteorological Institute for kindly providing unpublished SMB-projections for the Greenland ice sheet. Furthermore, a special thank goes to an anonymous friend and Ph.d-student from the centre for Ice and Climate, Niels Bohr Institute, for taking time to review parts of this thesis and provide very valuable feedback.

Bibliography

[1] Bamber, J. & Riva, R., 2010. The sea level fingerprint of recent ice massfluxes, Cryosphere, 4, 621–627, doi:10.5194/tc-4-621-2010.

[2] van den Broeke, M., Bamber, J., Ettema, J., Rignot, E., Schrama, E., van de Berg, W. J., van Meijgaard, E., Velicogna, I., and Wouters, B.: Partitioning Recent Greenland Mass Loss, Science, 326, 984–986, doi:10.1126/science.1178176, 2009.

[3] A. Cazenavea, O. Henrya, S. Muniera, T. Delcroixa, A. L. Gordonc, B. Meyssignaca, W. Llovelb, H. Palanisamya & M. Beckerd, Estimating ENSO Influence on the Global Mean Sea Level, 1993–2010, pages 82-97, DOI:10.1080/01490419.2012.718209

[4] Lawrence M. Cathles, 1975, Viscosity of the Earth's Mantle

[5] Church, J.A., P.U. Clark, A. Cazenave, J.M. Gregory, S. Jevrejeva, A. Levermann, M.A. Merri eld, G.A. Milne, R.S. Nerem, P.D. Nunn, A.J. Payne, W.T. Pfeffer, D. Stammer and A.S. Unnikrishnan, 2013: Sea Level Change. In: Climate Change 2013: The Physical Science Basis. Contribution of Working Group I to the Fifth Assessment Report of the Intergovernmental Panel on Climate Change [Stocker, T.F., D. Qin, G.-K. Plattner, M. Tignor, S.K. Allen, J. Boschung, A. Nauels, Y. Xia, V. Bex and P.M. Midgley (eds.)]. Cambridge University Press, Cambridge, United Kingdom and New York, NY, USA.

[6] Church, J. A. and N.J. White (2011), "Sea-level rise from the late 19th

to the early 21st Century", Surveys in Geophysics, 32(4-5), 585-602, doi:10.1007/s10712-011-9119-1.

[7] Farrell, W.E. & Clark, J.A., 1976. On postglacial sea-level, Geophys. J. R.astr. Soc., 46, 647–667

[8] X. Fettweis, B. Franco, M. Tedesco, J. H. van Angelen, J. T. M. Lenaerts, M. R. van den Broeke, and H. Galleé, 2013, Estimating the Greenland ice sheet surface mass balance contribution to future sea level rise using the regional atmospheric climate model MAR, The Cryosphere, 7, 469–489, 2013.

[9] J. J. Fuerst, H. Goelzer, and P. Huybrechts, 2015, Ice-dynamic projections of the Greenland ice sheet in response to atmospheric and oceanic warming, The Cryosphere, 9, 1039–1062, 2015

[10] Khan, S.A., Wahr, J., Stearns, L.A., Hamiltin, G.S., van Dam, T.,Larson, K.M. & Francis, O., 2007. Elastic uplift in southeast Green-land due to rapid ice mass loss, Geophys. Res. Lett., 34, L21701,doi:10.129/2007GL031468

[11] Kjeldsen, K.K., Korsgaard, N.J., Bjørk, A.A., Khan, S.A., Box, J.E., Funder, S., Larsen, N.K., Bamber, J.L., Colgan, W., van den Broeke, M., Siggaard-Andersen, M.-L., Nuth, C., Schomacker, A., Andresen, C.S., Willerslev, E. & Kjær, K.H. 2015, 'Spatial and temporal distribution of mass loss from the Greenland Ice Sheet since AD 1900' Nature, vol 528, pp. 396-400., 10.1038/nature16183

[12] Lambeck K, Chappell J (2001) Sea level change through the last glacial cycle. Science 292(5517):679–686.

[13] Lemke, P., J. Ren, R.B. Alley, I. Allison, J. Carrasco, G. Flato, Y. Fujii, G. Kaser, P. Mote, R.H. Thomas and T. Zhang, 2007: Observations: Changes in Snow, Ice and Frozen Ground. In: Climate Change 2007: The Physical Science Basis. Contribution of Working Group I to the Fourth Assessment Report of the Intergovernmental Panel on Climate

Change [Solomon, S., D. Qin, M. Manning, Z. Chen, M. Marquis, K.B. Averyt, M. Tignor and H.L. Miller (eds.)]. Cambridge University Press, Cambridge, United Kingdom and New York, NY, USA.

[14] Mauz, B.; Vacchi, M.; Green, A.; Hoffman, G.; Cooper, A. (2015) – Beachrock: A tool for reconstructing relative sea level in the far field. Marine Geology, 362(1):1-16. DOI: 10.1016/j.margeo.2015.01.009

[15] Meier, M.F., M.B. Dyurgerov, U.K. Rick, S. O'Neel, W.T. Pfeffer, R.S. Anderson, S.P. Anderson, and A.F. Glazovsky. 2007. Glaciers dominate eustatic sea-level rise in the 21st century. Science 317: 1064-1067.

[16] Mitrovica, J. X. & Peltier, W. R., 1991. On postglacial geoid subsidence over the equatorial ocean. J. geophys. Res., 96, 20,05320,071.

[17] Mitrovica, J. X., Tamisiea, M. E., Davis, J. L., and Milne, G. A.: Recent mass balance of polar ice sheets inferred from patterns of global sea-level change, Nature, 409, 1026–1029, 2001.

[18] Mitrovica J.X., Wahr J., Matsuyama I., Paulson A. The rotational stability of an ice-age earth. Geophys. J. Int. 2005;161:491-506.

[19] Nakada M., Okuno J., Lambeck K., Purcell A. Viscosity structure of Earth's mantle inferred from rotational variations due to GIA process and recent melting events. Geophys. J. Int. 2015;202:976-992.

[20] Nielsen, K., Sørensen, L. S., Khan, S. A., Spada, G., Simonsen, S. B., & Forsberg, R. (2014). Towards Constraining Glacial Isostatic Adjustment in Greenland Using ICESat and GPS Observations. In C. Rizos, & P. Willis (Eds.), Earth on the Edge: Science for a Sustainable Planet. (pp. 325-331). Springer.

[21] W.R. Peltier and J.T. Andrews, 1976, Glacial Isostatic Adjustment I: the Forward Problem, Geophys. J. Roy astr. Soc., 46, 605-646.

[22] W.R. Peltier, 2004. Global Glacial Isostasy and the Surface of the Ice-

Age Earth: The ICE-5G (VM2) Model and GRACE, Ann. Rev. Earth and Planet. Sci., 32, 111-149.

[23] W.R. Peltier, Argus, D.F. and Drummond, R. (2015) Space geodesy constrains ice-age terminal deglaciation: The global ICE-6G_C (VM5a) model. J. Geophys. Res. Solid Earth, 120, 450-487, doi:10.1002/2014JB011176.

[24] Perrette, M., F. Landerer, R. Riva, K. Frieler, and M. Meinshausen, 2013: A scaling approach to project regional sea level rise and its uncertainties. Earth Syst. Dyn., 4, 11–29, doi:10.5194/ esd-4-11-2013.

[25] Sella, G.F., Stein, S., Dixon, T.H., Craymer, M., James, T.S., Mazzotti, S. and Dokka, R.K. (2007). Observation of glacial isostatic adjustment in "stable" North America with GPS. Geophysical Research Letters 34: doi: 10.1029/2006GL027081. issn: 0094-8276.

[26] Spada, G., Stocchi, P, 2006, The Sea Level Equation: Theory and Numerical Examples.

[27] Spada G, Stocchi P (2007) SELEN: a Fortran 90 program for solving the "Sea Level Equation", Comput. and Geosci. 33(4):538–562. doi: 10.1016/j.cageo.2006.08.006

[28] Spada, G., G. Ruggieri, L. S. Sorensen, K. Nielsen, D. Melini, and F. Colleoni (2012), Greenland uplift and regional sea level changes from ICESat observations and GIA modelling, Geophys. J. Int., 189 (3), 1457–1474.

[29] Stocchi, P., Spada, G., Cianetti, S., 2005. Isostatic rebound following the Alpine deglaciation: impact on the sea level variations and vertical movements in the Mediterranean region. Geophysical Journal International 162, 137. doi:10.1111/j.1365-246X.2005.02653.x.

[30] Soerensen, L.S., 2010. Changes of the Greenland ice sheet derived fromICESat and GRACE data, PhD thesis, University of Copenhagen

[31] Sørensen LS, Simonsen SB, Nielsen K, Lucas-Picher P, Spada G, Adalgeirsdottir G, Forsberg R, Hvidberg CS (2011) Mass balance of the Greenland ice sheet (2003–2008) from ICESat data the impact of interpolation, sampling and firn density. Cryosphere 5(1):173–186. doi:10.5194/tc-5-173-2011

[32] Timmen, L., Gitlein, O., Klemann, V., and Wolf, D.: Observing gravity change in the Fennoscandian uplift area with the Hanover absolute gravimeter, Pure Appl. Geophys., 196, 1331– 1342, doi:10.1007/s00024-011-0397-9, 2011.

[33] Waelbroeck, C., L. Labeyrie, E. Michel, J. C. Duplessy, J. McManus, K. Lambeck, E. Balbon, and M. Labracherie (2002), Sea-level and deep water temperature changes derived from benthic foraminifera isotopic records, Quat. Sci. Rev., 21(1), 295–305.

[34] Woodward, R. S.: On the form and position of mean sea level, US Geol. Surv. Bull., 87–170, 1888.

[35] Yan, Q., H. J. Wang, O. M. Johannessen, and Z. S. Zhang, 2014: Greenland ice sheet contribution to future global sea level rise based on CMIP5 models. Adv. Atmos. Sci., 31(1), 8–16, doi: 10.1007/s00376-013-3002-6.

[36] Aagren, J. and Svensson, R.: Postglacial Land Uplift Model and System Definition for the New Swedish Height System RH 2000. LMV-Rapport 2007:4. Reports in Geodesy and Geographical In- formation Systems, Gaevle, ISSN 280-5731, 2007.

Appendix A

SELEN configuration file

Example input: IM45e

config.dat

```
!!!!!!!!!!!!!!!!!!!!!!!!!!!!!!!!!!!!!!!!!!!!!!!!!!!!!
  This is file "config.dat" for SELEN 2.9 -
!!!!!!!!!!!!!!!!!!!!!!!!!!!!!!!!!!!!!!!!!!!!!!!!!!!!!

~~~~~~~~~~~~~~~~~~~~~~~~~~~~~~~~~~~~~~~~~~~~~~~~~~~~~~~~~~~~~~~~~~~~~~~~~~~~~~~~~~~~~~~~~~~~~~~~~
The user can configure SELEN by the switches below. Any option is to be written within primes
e. g., 'option'. A three-digits, left aligned numerical code is provided for each entry e.g., 001.

In section 1 settings the user supplies the spatial resolution, the ice sheets distribution,
and the Earth model viscoelastic structure. This allows one to solve the Sea Level Equation but
no graphical output is obtained.

In section 2 outputs, a number of optional outputs can be scheduled, including tables and plots
of numerical results. The required GMT scripts are automatically generated according to the
options chosen.

For help, comments, or suggestion, you  can contact the authors at the addresses below or consult
the SELEN web page at http://geodynamics.org/cig/software/selen
```

```
Contact: Giorgio Spada <giorgio DOT spada AT gmail DOT com>
~~~~~~~~~~~~~~~~~~~~~~~~~~~~~~~~~~~~~~~~~~~~~~~~~~~~~~~~~~~~~~~~~~~~~~~~~~~~~~~~~~~~~~~~~~~~~

!!!!!!!!!!!!!!!!!!!!!!!!!!!!!!!!!!!!!!!!!!!!!!!!!!!!!
 This is SECTION 1 of "config.dat": SELEN settings
!!!!!!!!!!!!!!!!!!!!!!!!!!!!!!!!!!!!!!!!!!!!!!!!!!!!!

====> PURGING option ---------------------------------------------------------------
110  Purging the wdir before & after execution                      'y'
     [see config.f90 for purged filenames extensions ]

====> SOLUTION of the SLE ----------------------------------------------------------
130    Iterations & mode of solution                              '3'    '1'
Modes:  1= Gravitationally self-consistent GSC
        2= Elastic GSC / 3="Eustatic" / 4="Woodward" / 5="No Ice"

====> MAXIMUM HARMONIC DEGREE -----------------------------------------------------
140    LMAX                                                            '128'

====> REFERENCE FRAME -------------------------------------------------------------
145    Includes degree 1 Love numbers CM/CE frames             'y'  'CM'

====> TEGMARK RESOLUTION ----------------------------------------------------------
150    R                                                               '44'
151    Prepare a new pixel table y/n, filename         'y' 'px-table-r44.dat'

====> RHEOLOGICAL MODEL -----------------------------------------------------------
160    Rheological profile info:                            '3' '2' 'vsc_VM2a.dat'

====> ICE MODEL -------------------------------------------------------------------
170    Ice file name                                               'ice5g_im45.dat'
171    Prepare a new SH ice file y/n, filename       'y'  'ice5g-l128.dat'
172    Ice history time step kyrs                           '0.01'

====> SPHERICAL HARMONICS SH FILE AT PIXELS -------------------------------
180    A new SH file y/n, filename                    'y'  'sh-r44-l128.bin'

====> OCEAN FUNCTION OF ----------------------------------------------------
190    A new OF SH decomposition y/n, filename         'y'  'of-l128.dat'
```

```
====> REPOSITORY LABEL ---------------------------------------------------------
195    The depot name  four characters                 'IM45'

!!!!!!!!!!!!!!!!!!!!!!!!!!!!!!!!!!!!!!!!!!!!!!!!!!!!
 This is SECTION 2 of "config.dat: SELEN outputs
!!!!!!!!!!!!!!!!!!!!!!!!!!!!!!!!!!!!!!!!!!!!!!!!!!!!

====> EXECUTION of the GMT SCRIPTS ---------------------------------------------
200    Execution of GMT scripts during the SELEN run y/n     'n'

====> PIXELIZATION & WINDOW ----------------------------------------------------
205    Pixelization maps y/n                                  'y'
206    Window function evaluation & plot y/n                     'n'

====> OCEAN FUNCTION OF --------------------------------------------------------
210    Present-day OF map & reconstruction y/n                'y'
215    Plot of OF degree variance y/n                            'n'

====> ICE MODEL ----------------------------------------------------------------
220    Maps of original ice sheets  y/n                                'y'
221    Plot of Equivalent Sea Level ESL  y/n                              'y'
222    Reconstruction & mapping of the ice sheets y/n               'n'

====> EARTH MODEL SPECTRAL PROPERTIES ------------------------------------------
230    Plot LDCs, relaxation spectrum & residues for normal modes  y/n   'y'

====> RSL PREDICTIONS AT SPECIFIC SITES ----------------------------------------
240    RSL analysis, database & format                'y'  'sealevel.dat'   '0'
241    Plot of RSL sites distribution                          'y'
242    Site-by-site RSL predictions vs data & plots          'y'  'y'
243    Scatterplot of RSL data & predictions                   'y'
244    Misfit between RSL data & predictions               'n'
245    Table with all RSL data & predictions              'y'

====> RSL REGIONS --------------------------------------------------------------
250    Gobal RSL zones                                      'n'
251    Regional RSL contour lines                            'y'   'rsl-region.dat'
```

```
====> SEA LEVEL CHANGE AT TIDE-GAUGE STATIONS --------------------------------
260    Tide-gauge TG analysis & database                    'y' 'rlr-trends.txt'
261    Plot of TG stations distribution                      'y'
262    TG data scatterplot                                       'n'
263    Table of S, N, and U-dot predictions at TG sites    'y'

====> GLOBAL PRESENT-DAY RATES -----------------------------------------------
270    Global maps of dot S, U & N                          'y'

====> 3D VELOCITY ------------------------------------------------------------
275    -Up, North, East, S, and N rates for sites in file       'n' 'NA_KK.txt'

====> REGIONAL PRESENT-DAY RATES ---------------------------------------------
280    Regional maps of dot S, U, & N                     'n'
281      -1 Italy                                    'y'
282      -2 Mediterranean                              'y'
283      -3 Europe                                       'y'
284      -4 Fennoscandia                               'y'
285      -5 Greenland                                'y'
286      -6 North America                                'y'
287      -7 Antarctica                                 'y'

====> STOKES COEFFICIENTS SC -------------------------------------------------
290    Rate of change of SC & range of degrees for plot      'y'  '2'  '20'
```

DTU Space
National Space Institute
Technical University of Denmark

Elektrovej, building 327
DK - 2800 Kgs. Lyngby
Tel (+45) 4525 9500
Fax (+45) 4525 9575

www.space.dtu.dk